



THE UNIVERSITY *of* EDINBURGH

Edinburgh Research Explorer

Noncontrast Chest Computed Tomographic Imaging of Obesity and the Metabolic Syndrome

Citation for published version:

Representing the International Workshop for Pulmonary Functional Imaging (IWPF), Schlett, CL, Nattenmüller, J, Tsuchiya, N, Vogel-Claussen, J, Kauczor, H-U, Levin, D, Hatabu, H, Estépar, RSJ, Wu, M-T, van Beek, E & Schiebler, ML 2019, 'Noncontrast Chest Computed Tomographic Imaging of Obesity and the Metabolic Syndrome: Part I Cardiovascular Findings', *Journal of Thoracic Imaging*, vol. 34, no. 2, JTI-18-133R1. <https://doi.org/10.1097/RTI.0000000000000391>

Digital Object Identifier (DOI):

[10.1097/RTI.0000000000000391](https://doi.org/10.1097/RTI.0000000000000391)

Link:

[Link to publication record in Edinburgh Research Explorer](#)

Document Version:

Peer reviewed version

Published In:

Journal of Thoracic Imaging

General rights

Copyright for the publications made accessible via the Edinburgh Research Explorer is retained by the author(s) and / or other copyright owners and it is a condition of accessing these publications that users recognise and abide by the legal requirements associated with these rights.

Take down policy

The University of Edinburgh has made every reasonable effort to ensure that Edinburgh Research Explorer content complies with UK legislation. If you believe that the public display of this file breaches copyright please contact openaccess@ed.ac.uk providing details, and we will remove access to the work immediately and investigate your claim.



Journal of Thoracic Imaging

Non-Contrast Chest Computed Tomographic Imaging of the Metabolic Syndrome (MetS): Part I Cardiovascular Findings --Manuscript Draft--

Manuscript Number:	JTI-18-133R1
Full Title:	Non-Contrast Chest Computed Tomographic Imaging of the Metabolic Syndrome (MetS): Part I Cardiovascular Findings
Article Type:	Review Article (Invited)
Section/Category:	Cardiovascular (cardiac/aortic diseases)
Keywords:	Metabolic Syndrome Computed Tomography Coronary artery Calcification
Corresponding Author:	Mark L. Schiebler, M.D. University of Wisconsin-Madison Madison, Wisconsin UNITED STATES
Corresponding Author's Institution:	University of Wisconsin-Madison
Order of Authors:	Christopher L. Schlett, M.D., M.P.H. Johanna Nattenmüller, MD Nanae Tsuchiya, M.D., PhD Jens Vogel-Claussen, MD Hans-Ulrich Kauczor, MD David L. Levin, M.D., PhD Hiroto Hatabu, M.D., PhD Jose Raul Estépar, MD Ming-Ting Wu, MD Edwin J.R. van Beek, M.D., PhD Mark L. Schiebler, M.D.
Manuscript Region of Origin:	UNITED STATES
Abstract:	<p>There are physiological consequences of overeating that can lead to increased morbidity and mortality. Purpose of this review article is to acquaint the reader with the current state of the art in the non-cardiac gated, non-contrast chest Computed Tomographic (NCCT) imaging biomarkers of the metabolic syndrome (MetS) and their prognostic significance found in the lower neck and chest. NCCT Imaging biomarkers, associated with MetS in the chest include premature coronary artery calcification, acceleration of large vessel arterial and valvular calcifications associated with atherosclerosis, and pulmonary arterial enlargement from pulmonary hypertension associated with sleep apnea. These easily identified imaging biomarkers have prognostic implications for Major Adverse Cardiac Events (MACE). These NCCT chest-imaging biomarkers are likely targets for artificial intelligence algorithms to harvest for longitudinal assessment of their individual and multifactorial contributions to chronic disease, MACE and mortality. Early recognition and treatment of these common disorders may help improve patient outcomes and quality of life while decreasing medical costs.</p>

Joseph Schoepf, M.D.

Editor in Chief, Journal of Thoracic Imaging

Re: R1 JT1-18-133

Title: NON-CONTRAST CHEST COMPUTED TOMOGRAPHY OF OBESITY AND THE METABOLIC SYNDROME (METS): PART I CARDIOVASCULAR FINDINGS

Dear Dr. Schoepf,

Thank you for the opportunity to participate in the JTI Special Issue for January 2019.

We have made the suggested changes in the manuscript according to your and the reviewer comments.

Each comment is listed in order below. Our responses and changes in the manuscript put into are highlighted in yellow. We have changed the title slightly so that Part I and Part 2 have the same wording. Specifically the two words "Obesity and" have been added. We also added a supplemental figure from Raul Estepar's group on segmenting the left ventricle on non contrast non gated chest CT exams.

Reviewer #1:

1. Please name NCCT as Non contrast chest computed tomography in the abbreviation page.

Done

NCCT	Non contrast Computed Tomography
------	----------------------------------

2. In Heart and Valves Section - "...While all cardiac structures are affected by cardiac motion, there is increasing evidence that, with newer hardware low-dose NG-NCCT cardiac motion is less of a problem for calcification and myocardial scar assessment/quantification..) Please use the relevant references to support the mentioned evidence. Equally importantly please ensure that motion artefact especially in the assessment of small anatomical structures as coronary arteries, coronary artery calcifications can be influenced by heart rate dependent motion artefact and also the chosen CT protocol.

Good point here. We have added the following.

While all cardiac structures are affected by cardiac motion, there is increasing evidence that, with newer hardware, and faster gantry rotation times, low-dose NG-NCCT cardiac motion is less of a problem for calcification and myocardial scar assessment/quantification (Figures 1-4).(12-15)

3. In Coronary Artery Calcification section - It is proper to use the reference of Wu et al about the correlation between gated and non gated CT protocol based coronary calcium assessment. The authors mentioned an explanation that the quoted good correlation is due to thinner slice reconstruction which is misleading. The referenced article from 2008 used 16 slice MDCT with a mean heart rate of around 61beats/min. Thus it is important to emphasize in the presented review the importance of potential heart rate dependent motion artefact that can limit potentially significantly the accurate quantification of calcium score using non gated CT protocols.

We have added the following:

In a study by Wu et al (28) on 483 patients showed excellent correlation of Agatston CAC scores between a dedicated cardiac gated non-contrast CT for calcium scoring (16 slice multidetector, 3.0 mm slice thickness) and a low dose NG-NCCT (16 slice multidetector, 0.75mm slice thickness)performed for lung cancer screening (Figure 1). In their cohort of NG-NCCT patients the average heart was 61 beats per minute. They did not assess the importance of potential heart rate dependent motion artifact that may limit the accurate quantification of calcium score using non gated CT protocols.(28)

4. It would be beneficial to have a section of Radiation since the presented evidence may support potential CT screening for patients with Metabolic Syndrome.

We have added the following:

Radiation dose and safety using NG-NCCT for the diagnosis of MetS

We are not proposing to use NCCT for the diagnosis of MetS or obesity. From studies performed for other indications, the imaging physician can also make inferences about the metabolic milieu of that subject based on the multiple imaging findings discussed in this review. For the most, part low dose chest CT protocols are very low contributors to the medical radiation any patient receives over the course of their lifetime.(78) Each scan delivers between 0.5 and 5 mSv depending on the patient size, use of dose lowering reconstruction methods and automatic exposure control (limit mAs).(79)

EDITOR COMMENTS:

Editor in Chief comments: Add these references.

These references have been added to the manuscript.

1: Tabari A, Lo Gullo R, Murugan V, Otrakji A, Digumarthy S, Kalra M. Recent Advances in Computed Tomographic Technology: Cardiopulmonary Imaging Applications. J Thorac Imaging. 2017 Mar;32(2):89-100. doi: 10.1097/RTI.0000000000000258. Review. PubMed PMID: 28221262.

2: Renapurkar RD, Shrikanthan S, Heresi GA, Lau CT, Gopalan D. Imaging in Chronic Thromboembolic Pulmonary Hypertension. J Thorac Imaging. 2017 Mar;32(2):71-88. doi: 10.1097/RTI.0000000000000256. Review. PubMed PMID: 28060193.

3: Jivraj K, Bedayat A, Sung YK, Zamanian RT, Haddad F, Leung AN, Rosenberg J, Guo HH. Left Atrium Maximal Axial Cross-Sectional Area is a Specific Computed Tomographic Imaging Biomarker of World Health Organization Group 2 Pulmonary Hypertension. J Thorac Imaging. 2017 Mar;32(2):121-126. doi: 10.1097/RTI.0000000000000252. PubMed PMID: 28009778.

Joseph Schoepf, M.D.

Editor in Chief, Journal of Thoracic Imaging

Re: R1 JT1-18-133

Title: NON-CONTRAST CHEST COMPUTED TOMOGRAPHY OF OBESITY AND THE METABOLIC SYNDROME (METS): PART I CARDIOVASCULAR FINDINGS

Dear Dr. Schoepf,

Thank you for the opportunity to participate in the JTI Special Issue for January 2019.

We have made the suggested changes in the manuscript according to your and the reviewer comments.

Each comment is listed in order below. Our responses and changes in the manuscript put into are highlighted in yellow. We have changed the title slightly so that Part I and Part 2 have the same wording. Specifically the two words "Obesity and" have been added. We also added a supplemental figure from Raul Estepar's group on segmenting the left ventricle on non contrast non gated chest CT exams.

Reviewer #1:

1. Please name NCCT as Non contrast chest computed tomography in the abbreviation page.

Done

NCCT	Non contrast Computed Tomography
------	----------------------------------

2. In Heart and Valves Section - "...While all cardiac structures are affected by cardiac motion, there is increasing evidence that, with newer hardware low-dose NG-NCCT cardiac motion is less of a problem for calcification and myocardial scar assessment/quantification..) Please use the relevant references to support the mentioned evidence. Equally importantly please ensure that motion artefact especially in the assessment of small anatomical structures as coronary arteries, coronary artery calcifications can be influenced by heart rate dependent motion artefact and also the chosen CT protocol.

Good point here. We have added the following.

While all cardiac structures are affected by cardiac motion, there is increasing evidence that, with newer hardware, and faster gantry rotation times, low-dose NG-NCCT cardiac motion is less of a problem for calcification and myocardial scar assessment/quantification (Figures 1-4).(12-15)

3. In Coronary Artery Calcification section - It is proper to use the reference of Wu et al about the correlation between gated and non gated CT protocol based coronary calcium assessment. The authors mentioned an explanation that the quoted good correlation is due to thinner slice reconstruction which is misleading. The referenced article from 2008 used 16 slice MDCT with a mean heart rate of around 61beats/min. Thus it is important to emphasize in the presented review the importance of potential heart rate dependent motion artefact that can limit potentially significantly the accurate quantification of calcium score using non gated CT protocols.

We have added the following:

In a study by Wu et al (28) on 483 patients showed excellent correlation of Agatston CAC scores between a dedicated cardiac gated non-contrast CT for calcium scoring (16 slice multidetector, 3.0 mm slice thickness) and a low dose NG-NCCT (16 slice multidetector, 0.75mm slice thickness)performed for lung cancer screening (Figure 1). In their cohort of NG-NCCT patients the average heart was 61 beats per minute. They did not assess the importance of potential heart rate dependent motion artifact that may limit the accurate quantification of calcium score using non gated CT protocols.(28)

4. It would be beneficial to have a section of Radiation since the presented evidence may support potential CT screening for patients with Metabolic Syndrome.

We have added the following:

Radiation dose and safety using NG-NCCT for the diagnosis of MetS

We are not proposing to use NCCT for the diagnosis of MetS or obesity. From studies performed for other indications, the imaging physician can also make inferences about the metabolic milieu of that subject based on the multiple imaging findings discussed in this review. For the most, part low dose chest CT protocols are very low contributors to the medical radiation any patient receives over the course of their lifetime.(78) Each scan delivers between 0.5 and 5 mSv depending on the patient size, use of dose lowering reconstruction methods and automatic exposure control (limit mAs).(79)

EDITOR COMMENTS:

Editor in Chief comments: Add these references.

These references have been added to the manuscript.

1: Tabari A, Lo Gullo R, Murugan V, Otrakji A, Digumarthy S, Kalra M. Recent Advances in Computed Tomographic Technology: Cardiopulmonary Imaging Applications. *J Thorac Imaging*. 2017 Mar;32(2):89-100. doi: 10.1097/RTI.0000000000000258. Review. PubMed PMID: 28221262.

2: Renapurkar RD, Shrikanthan S, Heresi GA, Lau CT, Gopalan D. Imaging in Chronic Thromboembolic Pulmonary Hypertension. *J Thorac Imaging*. 2017 Mar;32(2):71-88. doi: 10.1097/RTI.0000000000000256. Review. PubMed PMID: 28060193.

3: Jivraj K, Bedayat A, Sung YK, Zamanian RT, Haddad F, Leung AN, Rosenberg J, Guo HH. Left Atrium Maximal Axial Cross-Sectional Area is a Specific Computed Tomographic Imaging Biomarker of World Health Organization Group 2 Pulmonary Hypertension. *J Thorac Imaging*. 2017 Mar;32(2):121-126. doi: 10.1097/RTI.0000000000000252. PubMed PMID: 28009778.

**Title: Non-Contrast Chest Computed Tomographic Imaging of Obesity and the Metabolic Syndrome (MetS):
Part I Cardiovascular Findings**

Authors: Christopher L. Schlett, MD MPH (1,2); Johanna Nattenmüller, MD (1,2); Nanae Tsuchiya, MD PhD (3,4); Jens Vogel-Claussen, MD (5); Hans-Ulrich Kauczor, MD (1,2); David Levin, MD PhD(6); Hiroto Hatabu, MD PhD FACR (7); Jose Raul Estépar, MD (8); Ming-Ting Wu, MD (9,10); Edwin J.R. van Beek, MD PhD (11) and Mark L. Schiebler MD (4)

Representing the International Workshop for Pulmonary Functional Imaging (IWPMI)

Author Affiliations:

1. Department of Diagnostic and Interventional Radiology, University Hospital of Heidelberg, Heidelberg, Germany.
2. Translational Lung Research Center (TLRC) Heidelberg, Member of the German Center for Lung Research (DZL), Heidelberg, Germany.
3. Department of Radiology, Graduate School of Medical Science, University of the Ryukyus, Okinawa 903-0215, Japan
4. Department of Radiology, University of Wisconsin-Madison, Madison, WI, USA
5. Department of Radiology, University Hospital Hannover, Germany
6. Department of Radiology, Mayo Clinic, Rochester, Minnesota, USA
7. Department of Radiology, Brigham and Women's Hospital and Harvard Medical School, Boston, MA, USA
8. Department of Pulmonary Medicine, Brigham and Women's Hospital and Harvard Medical School, Boston, MA, USA
9. Department of Radiology, Kaohsiung Veterans General Hospital, Kaohsiung, Taiwan
10. Faculty of Medicine, School of Medicine, National Yang-Ming University, Taipei, Taiwan
11. Edinburgh Imaging, Queen's Medical Research Institute, University of Edinburgh, Edinburgh, UK

Corresponding Author:

Mark L. Schiebler, M.D.
Professor of Radiology
UW-Madison School of Medicine and Public Health
600 Highland Avenue
Madison, Wisconsin
Telephone: 608-263-1229
Fax:
Email: mschiebler@uwhealth.org

**Title: Non-Contrast Chest Computed Tomographic Imaging of Obesity and the Metabolic Syndrome (MetS):
Part I Cardiovascular Findings**

Authors: Christopher L. Schlett, MD MPH (1,2); Johanna Nattenmüller, MD (1,2); Nanae Tsuchiya, MD PhD (3,4); Jens Vogel-Claussen, MD (5); Hans-Ulrich Kauczor, MD (1,2); David Levin, MD PhD(6); Hiroto Hatabu, MD PhD FACR (7); Jose Raul Estépar, MD (8); Ming-Ting Wu, MD (9,10); Edwin J.R. van Beek, MD PhD (11) and Mark L. Schiebler MD (4)

Representing the International Workshop for Pulmonary Functional Imaging (IWPF)

Author Affiliations:

1. Department of Diagnostic and Interventional Radiology, University Hospital of Heidelberg, Heidelberg, Germany.
2. Translational Lung Research Center (TLRC) Heidelberg, Member of the German Center for Lung Research (DZL), Heidelberg, Germany.
3. Department of Radiology, Graduate School of Medical Science, University of the Ryukyus, Okinawa 903-0215, Japan
4. Department of Radiology, University of Wisconsin-Madison, Madison, WI, USA
5. Department of Radiology, University Hospital Hannover, Germany
6. Department of Radiology, Mayo Clinic, Rochester, Minnesota, USA
7. Department of Radiology, Brigham and Women's Hospital and Harvard Medical School, Boston, MA, USA
8. Department of Pulmonary Medicine, Brigham and Women's Hospital and Harvard Medical School, Boston, MA, USA
9. Department of Radiology, Kaohsiung Veterans General Hospital, Kaohsiung, Taiwan
10. Faculty of Medicine, School of Medicine, National Yang-Ming University, Taipei, Taiwan
11. Edinburgh Imaging, Queen's Medical Research Institute, University of Edinburgh, Edinburgh, UK

Corresponding Author:

Mark L. Schiebler, M.D.
Professor of Radiology
UW-Madison School of Medicine and Public Health
600 Highland Avenue
Madison, Wisconsin
Telephone: 608-263-1229
Fax:
Email: mschiebler@uwhealth.org

Non-Contrast Chest Computed Tomographic Imaging of Obesity and the Metabolic Syndrome (MetS): Part 1 Cardiovascular Findings

Abstract

There are physiological consequences of overeating that can lead to increased morbidity and mortality. Purpose of this review article is to acquaint the reader with the current state of the art in the non-cardiac gated, non-contrast chest Computed Tomographic (NCCT) imaging biomarkers of the metabolic syndrome (MetS) and their prognostic significance found in the lower neck and chest. NCCT Imaging biomarkers, associated with MetS in the chest include premature coronary artery calcification, acceleration of large vessel arterial and valvular calcifications associated with atherosclerosis, and pulmonary arterial enlargement from pulmonary hypertension associated with sleep apnea. These easily identified imaging biomarkers have prognostic implications for Major Adverse Cardiac Events (MACE). These NCCT chest-imaging biomarkers are likely targets for artificial intelligence algorithms to harvest for longitudinal assessment of their individual and multifactorial contributions to chronic disease, MACE and mortality. Early recognition and treatment of these common disorders may help improve patient outcomes and quality of life while decreasing medical costs.

Key words (Mesh Terms): Humans, Biomarkers, Prognosis, Metabolic Syndrome, Tomography, X-ray computed, Calcium Scoring, Atherosclerosis, Sleep apnea syndrome, Pulmonary Hypertension, Thorax

Abbreviations:

AVC	Aortic Valve leaflet Calcification
CAC	Coronary Artery Calcification
CT	Computed Tomography
DSC Ca++	DeSCending aorta Calcium value
FR	Framingham Risk Score
HR	Hazard Ratio
HU	Hounsfield unit
LA	Left Atrium
LAD Ca++	Left Anterior Descending coronary artery Calcium value,
<u>LA-MACSA</u>	<u>Left atrial maximal cross-sectional area (mm²)</u>
LV	Left Ventricle
MAC	Mitral valve Annulus Calcification
MACE	Major adverse cardiovascular event
MV CA++	Mitral Valve leaflet Calcification
MetS	Metabolic Syndrome (a.k.a. Syndrome X)
<u>NCCT</u>	<u>Non contrast Computed Tomography</u>
NG-NCCT	Non cardiac Gated, Non-Contrast chest Computed Tomography
OSA	Obstructive Sleep Apnea
PH	Pulmonary Hypertension
mPAP	mean Pulmonary Artery Pressure
RV	Right Ventricle
TAC	Thoracic Aortic Calcification

Formatted: Superscript

Introduction

Cardiovascular disease (CVD) is the number one cause of mortality with an estimated 17.9 million deaths worldwide in 2015 (1). This represents an increasing problem for public health in both developed and developing countries (1). The metabolic syndrome (MetS) is a complex disorder of metabolism which results in an increased risk for CVD and Type 2 diabetes (2). It is comprised of a cluster of risk factors including elevated blood pressure, dyslipidaemia (lowered high-density lipoprotein (HDL) cholesterol and elevated triglycerides), elevated fasting glucose and central obesity (2). The American Heart Association/ ATP III definition of MetS is dependent on three of the five risk factors being present (2):

enlarged waist circumference with population-specific and country-specific criteria; triglycerides ≥ 150 mg/dL, HDL-c < 40 mg/dL in men and < 50 mg/dL in women, systolic blood pressure ≥ 130 mm Hg or diastolic blood pressure ≥ 85 mm Hg and fasting glucose > 100 mg/dL, with the inclusion of patients taking medication to manage hypertriglyceridemia, low HDL-c, hypertension and hyperglycemia.(2).

All parts of the body are affected by MetS. Recently, Bizino et al, reviewed the role of MRI for the study of MetS in the entire body.(3) Work on the gut-brain axis also shows that there is bidirectional signalling between the two organs and that the metabolome in the gut, which is influenced by a high fat/refined sugar diet, has critical roles in host metabolism, the brain reward system and behavior. (4) Put into more mundane terms, “the comfort foods of sugar and fat taste good and the brain wants more than the body needs.” This trend for overindulgence in food and sugar filled, and/or alcoholic drinks, spells trouble for the future of medical care expenditures in the developed world.

The underlying pathophysiology of MetS is related to the induction of low-grade systemic inflammation via increased levels of inflammatory cytokines (e.g. IL-6, IL-1 and TNF- α), adipokines and leptin, which originate from adipocytes or macrophages in the fat tissue. (5) This inflammatory process contributes to atherosclerosis, metabolic dysfunction and results in MetS. This increase in inflammation also effects the lung function by activation of

fibroblasts, endothelial cells of the lung vessels, airway epithelial and smooth muscle cells. This helps to explain why asthma is more severe in obese individuals. (5) Also, insulin resistance increases in asthmatics as insulin alters airway function and structure. (5) Obesity is thus associated with severe asthma induced by low-grade systemic inflammation and insulin resistance, which implies that strategies to treat insulin resistance, obesity and systemic inflammation could work also for asthma. (5, 6)

The prevalence of obesity in adults, defined as BMI >25.0 kg/m², has increased worldwide from 1980 to 2013: in women from 29.8 to 38.0 % and in men from 28.8 to 36.9 %. (7) This problem is not limited to the adult population, as childhood obesity has also become an increasing problem with important future consequences for public health expenditures, morbidity and mortality. (7) Reasons for this increase are high caloric diet, changes of diet composition, changes in microbiome of gut, changes in behaviour and lack of physical exercise. (7) In the developing countries, obesity increased from 8.4 to 13.4 in girls and from 8.1 to 12.9% in boys, while the proportion of obesity in the developed countries meanwhile is 22.6% in girls and 23.8 in boys. (7) As a consequence, cardiovascular dysfunction, diabetes or fatty liver disease with possible progression to end stage liver disease are apparent at an early age. (7-9) As the developed world ages, the health effects of obesity (MetS, Type 2 diabetes, cardiovascular disease and osteoarthritis of the spine, knees and hips) will demand an even larger portion of future public health expenditures.

The purpose of this review is to acquaint radiologists with the current state of the art in the non-cardiac gated, non-contrast chest computed tomography (NG-NCCT) cardiovascular imaging biomarkers found patients with obesity and the metabolic syndrome (MetS) and their prognostic significance. Our aim is to help identify those persons at risk using the metrics from these imaging biomarkers and to then recommend lifestyle interventions (weight reduction, increased physical activity and nutritional intervention) and a modification of medical management or surgery to improve patient outcomes. (10)

Heart and great vessels

The progression of cardiac and vascular disease takes place over decades and is for the most part asymptomatic. Thus, without testing the patient is not aware of the degree of his/her atherosclerotic burden. NG-NCCT can detect and quantify early heart disease and serve as a prognostic marker, particularly in patients with MetS. Madaj and Budoff published a nice summary of the risk stratification that NCCT can provide.(11) Given the limited soft-tissue contrast of non-enhanced CT, most prognostic markers are based on the quantification of calcification - either as part of vascular arteriosclerosis or valve leaflet calcification. While all cardiac structures are affected by cardiac motion, there is increasing evidence that, with newer hardware, and faster gantry rotation times, low-dose NG-NCCT cardiac motion is less of a problem for calcification and myocardial scar assessment/quantification (**Figures 1-4**).(12-15) Furthermore, arteriosclerosis is a systemic disease and although the association is stronger between atherosclerotic alteration and development of further events in the same organ segment (16), assessment of one vascular bed may serve as a proxy for an overall risk marker. However, a significant portion of potentially clinically significant cardiovascular findings are currently not mentioned in the written reports, particularly by junior radiologists.(17)

Coronary artery Calcification

The most important non-acute finding on NCCT predictive of future major adverse cardiac events is coronary artery calcification (CAC) (**Figures 2 and 4**). Broad evidence exists regarding the prognostic value of coronary artery calcification (CAC) for cardiovascular events (18-22). More importantly, the use of CAC improved risk stratification beyond existing, clinical risk scores. This was conclusively shown in the Heinz-Nixdorf RECALL included 4,487 subjects without known CAD. With the addition of CAC assessment to the Framingham-Risk-Score the area under the curve improved from 0.681 to 0.749 ($p<0.003$) and when CAC was added to the National Cholesterol Education Panel ATP III categories the area under the curve improved from 0.653 to 0.755 (18). CAC was a much stronger predictor of risk than carotid intima-media thickness, high-sensitivity C reactive protein and the ankle-brachial index (19). Further results from the MESA study showed that CAC improves risk assessment in individuals with family history (19). Consequently, CAC assessment has been incorporated into many clinical guidelines for risk stratification. Depending on the guideline used, CAC is considered an appropriate test to perform in asymptomatic adults at intermediate risk for heart disease. These patients are defined by having a 10%

to 20% 10-year risk or having a Systemic Coronary Risk evaluator (SCORE) (23) risk stratification value range of 5% - 10%, low-risk individuals with a family history of premature disease and all diabetic patients 40 years or older are also candidates for this test. (24-26) Budoff and colleagues (22) have recently shown that in the MESA cohort (N=6814) (<https://www.mesa-nhlbi.org/Calcium/input.aspx>) for each doubling of CAC there was a 14% increase in CVD risk. They concluded that CAC is highly associated with MACE and is this gated non contrast CT biomarker was found to be independent of standard risk factors (Supplementary Table S1).(22)

Evidence based guidelines for the use of CAC are based on publications using cardiac-gated CT. This is because CAC has a high density and is sensitive to motion artefacts leading to false CAC values (27). New technology of multi-detector computed tomography scanners with faster gantry rotation times and thinner detector row widths allow for thinner slices with a reduction in partial volume effects. These changes in hardware now allow for more exact and reliable measurement of CAC on non-gated NCCT scans (NG-NCCT). In a study by Wu et al (28) on 483 patients showed excellent correlation of Agatston CAC scores between a dedicated cardiac gated non-contrast CT for calcium scoring (16 slice multidetector, 3.0 mm slice thickness) and a low dose NG-NCCT (16 slice multidetector, 0.75mm slice thickness) performed for lung cancer screening (**Figure 1**). In their cohort of NG-NCCT patients the average heart was 61 beats per minute. They did not assess the importance of potential heart rate dependent motion artifact that may limit the accurate quantification of calcium score using non gated CT protocols.(28) They found an intraclass correlation coefficient of 0.95 for the agreement between the scores on low-dose NG-NCCT versus the respective routine cardiac-gated CT for CAC in this one observer study. In a study by Kim et al., where 128 patients underwent both non-gated low dose lung cancer screening and ECG-gated CAC scanning, an accuracy of 90% was observed for CAC>0 on the gated CAC scan and the absolute CAC scores correlated well (r=0.89) (29). In a meta-analysis of 661 subjects (3 separate studies) performed in 2013, Xie et al convincingly showed that, when the Agatston Score at non-gated low dose NCCT was compared with the gold standard of routine cardiac gated CT performed for CAC scoring, the pooled correlation coefficient was 0.94 (95%CI: 0.89-0.96). These data are confirmative of the newly available scatter plot from Wu et al(28) (**Figure 1**) showing a R² of 0.95 between Agatston scores as derived from NG-NCCT versus cardiac gated CT.

Formatted: Left

Formatted: Font: 10 pt

Formatted: Font: 10 pt

While the Agatston score as a continuous measurement has been established for formal CAC assessment, the development of visual scores for CAC categorization is essential in order to provide the chest radiologist with a simple technique that is less time consuming. Several studies have been performed showing that either a visual-qualitative assessment or a visual ordinal scale can be used for reliable and accurate risk assessment as compared to Agatston score (30-32). But more importantly, both Agatston score and/or a visual CAC assessment from NG-NCCT have prognostic value for cardiovascular events and overall mortality. In detail, a study performed by Mets et al in 3,648 lung cancer screening patients using an automatically derived Agatston score from NG-NCCT in a risk prediction model found overall good discrimination (AUC 0.71) with an event frequency of 12.2% vs 4.0% in the high vs. low risk groups, respectively.(33) In the ECLIPSE trial Williams et al found that CAC was increased in patients with chronic obstructive pulmonary disease and was associated with an increased risk of death.(34) In the National Lung Screening Trial assessing 1,442 patients (35), an Agatston scores of 1-100, 101-1000, and >1000 had HR of 1.27, 3.57, and 6.63 as derived from NG-NCCT and compared to an Agatston score of 0. Interestingly, in a case-control study authored by Hughes-Austin et al. in which both ECG-gated 3 mm and non-gated 6 mm CT scans were available, the predictive value of the Agatston score for mortality where similar.(36) Focusing on visual assessment, Shao et al showed in a single centre study that there is no significant difference in the discriminative power of visual CAC assessment vs. Agatston score (AUC: 0.80, 0.81).(37) Most evidence exist for a visual assessment using an ordinal CAC scoring system categorizing from 0-12 or 0-30 based upon visual estimation (**Table 1**). The study of Shemesh et al. including 8,782 smokers with 72 months mean follow up showed that this simple ordinal system was strongly predictive for cardiovascular death (32) and further confirmed by Blair et al. to be of similar predictive value as the Agatston score (31) (**Table 2**). Gonzales et al have recently shown that automated detection of Agatston scores can be derived from NG-NCCT exams.(38) Thus, in a common guideline, the Society of Cardiovascular Computed Tomography (SCCT) and the Society of Thoracic Radiology (STR) recommend “the incorporation of CAC into all non-gated non-contrast chest examination reports” since it “in the treatment of coronary artery disease”.(39)

It is very clear that coronary artery calcium can be reliably detected on NG-NCCT and that either ordinal scoring methods or quantification of the NG-NCCT Agatston score are highly correlated (within 10%) with those cardiac gated non-contrast CT exams that are performed only for CAC scoring. *An argument can be made that the*

CAC score value obtained using current state of the art multidetector NG- NCCT of the chest, performed for any reason, are a good proxy for a dedicated CAC scoring CT.

Aortic calcification

The thoracic aorta is another important vascular bed imaged on a standard chest CT. As compared to the coronary arteries, the assessment thoracic aorta calcification (TAC) less standardized but also less effected by cardiac motion. In a retrospective study by Jairam et al. found good predictive value for cardiovascular events when including visual assessment of TAC (HR: 0.37, $p < 0.001$) into a larger predicting model.(40) Similar results were observed in the Heinz Nixdorf RECALL study (41), where TAC together with other CT-derived parameters improved the prediction of events over the Framingham Risk Score and CAC (AUC: 0.749 to 0.764; $p = 0.01$). In contrast, Kim et al found in subjects from the MESA study without CAC ($n = 3,415$) that TAC was associated to cardiovascular events and all-cause mortality, but this association attenuated after adjustment for cardiovascular risk factors.(42) Similarly, in the Framingham Heart Study TAC provided no incremental value above risk factors for the prediction of events.(43) Thus, TAC is a prognostic marker, but its incremental value to traditional risk factors and other CT-findings, particular to CAC remain controversial.

Valvular Calcification

The most common valve affected by calcification is the aortic valve. The aortic valve calcification (AVC) can vary by its degree and/or by its location and can lead to aortic stenosis. The degree of stenosis is increasing with AVC extent, while calcification of the peripheral left-posterior and the central right-left commissural leaflets is particularly correlated with mean and peak gradient increases across the aortic valve.(44) The underlying pathophysiology is complex and integrates lipids, the renin-angiotensin system, inflammation, signalling pathways, and genetic predisposition.(45) Also, a strong linkage to visceral obesity has been described leading the neologism 'valvulo-metabolic' risk.(46) Further, AVC shares common risk factors with arteriosclerosis; hence, patients with AVC had more frequently coexisting presence of coronary plaque and had a greater extent of coronary plaque burden (6.4 vs 1.8 segments for patients with and without AVC, $P < 0.001$) as described in a study of 357 subjects undergoing cardiac

CT. (47) Interestingly, AVC was more strongly associated with calcified (OR: 5.2, $p=0.004$), then with mixed (OR: 3.2, $p=0.02$) or non-calcified plaque ($P=0.96$). Several studies have been performed regarding the prognostic value of AVC for cardiovascular events and all-cause mortality. Although AVC showed a prognostic value in univariate analysis, it attenuated in most studies after adjustment for traditional risk factors and after further adjustment for CAC and/or TAC.(43, 48-50)

Annular Calcification

The annulus of the mitral valve is most commonly calcified. Mitral annular calcification (MAC) is a chronic degenerative process in the fibrous base of the mitral valve and more commonly affects the posterior annulus than the anterior annulus. (51) Traditionally, MAC is assessed using echocardiography and several studies using this technology showed independent association of MAC with cardiac events.(52, 53) Given a good relationship in MAC between echocardiography and CT (54), MAC was also a good predictor for cardiovascular events if assessed by CT (55, 56). In the Northern Manhattan Study ($n=1,955$) (55), MAC prevalence was 27%, while severe MAC ($>4\text{mm}$ thickness) was observed in 13%. Presence of MAC was associated with myocardial infarction (HR: 1.75) and cardiac death (HR: 1.53) and these associations became stronger if using severe MAC as the predictor (HR: 1.89 and 1.81; respectively). In this cohort, but also in a cohort with atrial fibrillation, MAC was not significantly associated with cerebrovascular events. (55, 56)

Caseous calcification of the mitral valve is a rare form of MAC. The contents of the hollowed out cavity in the mitral valve annulus is composed of a mixture of calcium, fatty acids, and cholesterol that has a “toothpaste-like” texture. This commonly presents as an intracardiac mass at echocardiography. There is limited evidence regarding the prognostic value of caseous calcification of the mitral annulus. In a literature review of 1,502 articles, Dietl et al. identified a total of 130 patients with caseous calcification of the mitral annulus reported in 86 publications. The prevalence of cerebrovascular events was higher in patients with caseous calcification of the mitral annulus than with simple MAC (19% vs 12%, respectively; $p=0.02$).

Atrial and Ventricular size

There is a large body of evidence that MetS carries an increased risk of left ventricle (LV) hypertrophy, left atrial (LA) enlargement, systolic and/or diastolic dysfunction, arrhythmias and interstitial myocardial fibrosis. MetS is also associated with increased LV mass and LV diastolic dysfunction.(57, 58) ~~(Aijaz et al 2008, Ladeiras-Lopes et al. 2018, Shah et al. 2013)~~ CT can be useful for assessing cardiac chambers to determine their size, shape and thickness. Cardiac gated CT scans can usually be obtained during diastole for CAC scoring and coronary angiography, as this phase of the cardiac cycle has the least motion. While chamber assessment is relatively simple for gated, contrast-enhanced CT scans given existing software tools, NG-NCCT exams are more challenging and an area-based approach has been proposed. Schlett et al. showed that an area-based measurement for LV on axial, non-contrast enhanced CT images correlates well with LV volume, mass and size ($r=0.68$; $r=0.73$; $r=0.82$). (59) Similar correlations were observed for the left atrium.(60) In the MESA cohort, such area-based LV measurement of non-contrast CT scans is a predictor of incident heart failure events (HR 1.15; 95%CI 1.11-1.20) beyond traditional risk factors and CAC score; but also for CHD events (HR 1.07; 95%CI 1.03-1.10). As RV and LV contraction is usually synchronous, the RV/LV diameter and volume ratios have been used in NG-NCCT studies to assess RV dilation and dysfunction in response to increased RV afterload. (Henzler et al 2012, Mansencal et al. 2005) A limited number of reports indicate that RV hypertrophy may parallel alterations in LV structure and function in the setting of systemic hypertension, obesity and diabetes. (Chahal et al 2012) All the components of MetS (increased blood pressure, abdominal obesity, increased fasting glucose level and dyslipidemia) may induce right ventricular remodelling by several hemodynamic and non-hemodynamic mechanisms. (Tadic et al. 2013) Increasing evidence suggests that in pulmonary hypertension (PH) RV dysfunction is associated with various components of MetS, such as insulin resistance, hyperglycemia, and dyslipidemia. (Talati et al. 2015)

Regarding LA assessment, an enlarged size was associated with a 3- to 5-fold increase risk for ACS and provided incremental value for predicting ACS when added to the CT finding of indeterminate coronary artery stenosis in a population with acute chest pain presenting to the ED. (61) In the Heinz-Nixdorf Recall Study (62), LA size had prognostic value (HR 1.48), which remained significant after adjustment for traditional risk factors (HR 95%CI: 1.09-1.43) and after adjustment for traditional risk factors plus CAC (HR 95%CI: 1.07-1.40) (**Table 2**). Prognostic value of LA size was similar for different endpoints (coronary event: HR: 1.21; stroke: 1.31; CV death:

Formatted: Left, Space After: 0 pt, Don't adjust space between Latin and Asian text, Don't adjust space between Asian text and numbers

1.33). LA size also remained associated with cardiovascular events independent of other CT non-coronary findings.(41) Recently Jivraj et al have shown in 165 patients with right heart catheterization proven pulmonary hypertension (PAP > 45 mm Hg) and capillary wedge pressures (43 patients - PCWP > 15 mm Hg, 122 patients PCWP < 15 mm Hg) that left atrial maximal cross-sectional area (LA-MACSA) measured from NG-NCCT (LA-MACSA > 2400mm², P<0.001) had a 44% sensitivity and 93% specificity for pulmonary hypertension from left heart disease.(63) On NG-NCCT studies the images may not reveal the true ventricular morphology because the phase of the cardiac cycle is unknown. However, a few studies have reported good sensitivity and specificity (both >68%) of standard axial, non-gated chest CT for cardiomyopathies. (64) ▲

Formatted: Superscript

Formatted: Font: (Default) AdvTimes, 8 pt, English (United States)

Left ventricle

The left ventricle size (volume and in-plane area) can be estimated from NCCT chest exams. Bhatt and colleagues (65) have created an automated process for generating the expected ventricular sizes from NG-NCCT chest exams by comparing these studies to ultrasound and cardiovascular MRI exams that show the ventricular volumes and wall thickness (Supplemental Figure 1). The assessment of ventricular volume and wall thickness is easier if the patient is anemic, as the ventricular chambers are seen to be of lower Hounsfield unit density than the walls. The presence of prior left ventricular myocardial infarction is also easily determined by the presence of a low density scar (**Figure 3**). These are typically seen in the subendocardial regions of the wall and may be transmural.

Recently Kockelkoren et al published their data from routine NG-NCCT exams on patients that were studied for non-cardiovascular disease (**Tables 3 and 4**). This was derived from a rather homogeneous population of Caucasians in the United Kingdom. This group of researchers created a simple to use ordinal grading scale for the determination of future major adverse cardiac events (MACE) (**Table 3**) and have a computational model for the likelihood of a major cardiac event within 5 years that is based on a best fit multivariable regression model (**Supplementary Tables S2, S3**). The parameters include: age, male gender, indication for exam, left anterior descending coronary artery calcium (LAD Ca++) value, mitral valve leaflet calcification (MV CA++) value, descending aorta calcium value (DSC Ca++), and the maximum transverse diameter (cm) of the heart.

Epicardial Fat

In their study of 3,630 subjects from the Heinz-Nixdorf Recall Study, Mahabadi et al(41) found that the epicardial fat volume (HR: 1.15, 95% C.I 1.01-1.30, p value 0.03), was an imaging biomarker predictive of myocardial infarction, stroke and cardiovascular death (**Table 5**). In their systematic review, Bertaso et al found that the heterogeneity of the studies limits the conclusions that can be drawn from using this metric. They found that this visceral fat deposit is highly correlated with obesity, diabetes mellitus, age and hypertension. Manno et al showed that epicardial fat thickness at ultrasound was correlated with higher LDL cholesterol.(66) In their study from 2018, Hedgire et al show that perivascular fat stranding, seen on coronary CT angiography is associated with high risk clinical features and they suggest that fat stranding is a potential imaging biomarker of high-risk and/or ruptured atherosclerotic plaques.(67) Hartiala et al found no evidence that increased epicardial fat volume was independently associated with pre-clinical atherosclerosis.(68) Instead, they found that epicardial fat volume was primarily associated with BMI and waist circumference.(68) Furthermore, there is increasing evidence that fat quality rather fat volume may play a role in the association to CVD. (69)

Pulmonary artery diameter predicts pulmonary hypertension

Sleep disordered breathing (sleep apnea) is an important cause of pulmonary hypertension.(70) Obstructive Sleep Apnea (OSA) is caused by the increased collapsibility of the upper airway from loss of muscle tone and a decrease in the effective orifice from fat deposition in the tongue and surrounding pharynx during sleep.(71) This results in decreased or absent airflow and hypoxia. These episodes are usually terminated by a brief arousal from sleep and resulting in sleep deprivation for subjects with MetS.(72) Over many years, these apneic episodes lead to sleep fragmentation and altered cognitive function. (73) These episodes of hypoxia are associated with pulmonary artery vasoconstriction and can lead to permanent changes in PA size (**Figure 5**). (74) Corson et al studied 175 subjects with right heart catheterization (RHC) proven pulmonary hypertension (PH), 16 normal patients with proven normal mean pulmonary artery pressures (mPAP) and 114 subjects without known mPAP and found a sensitivity of the criterion “mean pulmonary artery diameter at the level of the bifurcation >29mm” was 0.89 (95% C.I. 0.84-0.93) and a specificity of 0.83 (95%CI: 0.76-0.90).(75) Truong et al studied 706 “healthy cohort” subjects in the Framingham Heart Study using cardiac gated NCCT and found a 90th percentile cut-off value of 28.9 mm in men and 26.9 mm in women.(76) Pulmonary artery diameter is an important clue that may indicate pulmonary

hypertension ~~from any cause~~ (77); ~~and in the setting of obesity or MetS an enlarged PA can then~~ be used to alert the imager and clinician to the possibility for OSA. Instituting treatment with Continuous Positive Airway Pressure (CPAP) can significantly improve the length and quality of life for these individuals.

Radiation dose and safety using NG-NCCT for the diagnosis of MetS

We are not proposing to use NCCT for the diagnosis of MetS or obesity. From studies performed for other indications, the imaging physician can also make inferences about the metabolic milieu of that subject based on the multiple imaging findings discussed in this review. For the most part low dose chest CT protocols are very low contributors to the medical radiation any patient receives over the course of their lifetime. (78) Each scan delivers between 0.5 and 5 mSv depending on the patient size, use of dose lowering reconstruction methods and automatic exposure control (limit mAs). (79)

Conclusion

The beauty of non-gated, non-contrast computed of the chest is that quantitative assessment of Hounsfield unit density, contour and volume of many organs can be assessed longitudinally and correlated to patient outcomes. This differs substantially from contrast enhanced CT data, because there is no iodinated contrast material confounding the density measurements. There are easy to access imaging biomarkers associated with obesity, atherosclerotic disease and MetS that are routinely seen on these exams. The most important one found on NG-NCCT is coronary artery calcification. Various models combining clinical and imaging data have been shown to have prognostic significance for Major Adverse Cardiac Events. Thus, these exams are a virtual treasure trove of quantitative imaging biomarker information available for retrospective analysis to create survival models (training sets) that can be applied prospectively to test sets and validated with external data sets. These big data can be added to radiomic feature analysis, convolutional neural networks and/or added to deep neural networks without any user defined features to create better survival models that can be used to help design personalized medical interventions aimed at prolonging quality life expectancy.

References

1. Mortality GBD, Causes of Death C. Global, regional, and national life expectancy, all-cause mortality, and cause-specific mortality for 249 causes of death, 1980-2015: a systematic analysis for the Global Burden of Disease Study 2015. *Lancet*. 2016;388(10053):1459-544.
2. Alberti KG, Eckel RH, Grundy SM, et al. Harmonizing the metabolic syndrome: a joint interim statement of the International Diabetes Federation Task Force on Epidemiology and Prevention; National Heart, Lung, and Blood Institute; American Heart Association; World Heart Federation; International Atherosclerosis Society; and International Association for the Study of Obesity. *Circulation*. 2009;120(16):1640-5.
3. Bizino MB, Sala ML, de Heer P, et al. MR of multi-organ involvement in the metabolic syndrome. *Magn Reson Imaging Clin N Am*. 2015;23(1):41-58.
4. de Clercq NC, Frissen MN, Groen AK, Nieuwdorp M. Gut Microbiota and the Gut-Brain Axis: New Insights in the Pathophysiology of Metabolic Syndrome. *Psychosom Med*. 2017;79(8):874-9.
5. Peters MC, Fahy JV. Metabolic consequences of obesity as an "outside in" mechanism of disease severity in asthma. *Eur Respir J*. 2016;48(2):291-3.
6. Peters MC, McGrath KW, Hawkins GA, et al. Plasma interleukin-6 concentrations, metabolic dysfunction, and asthma severity: a cross-sectional analysis of two cohorts. *Lancet Respir Med*. 2016;4(7):574-84.
7. Ng M, Fleming T, Robinson M, et al. Global, regional, and national prevalence of overweight and obesity in children and adults during 1980-2013: a systematic analysis for the Global Burden of Disease Study 2013. *Lancet*. 2014;384(9945):766-81.
8. Schwimmer JB. Definitive diagnosis and assessment of risk for nonalcoholic fatty liver disease in children and adolescents. *Semin Liver Dis*. 2007;27(3):312-8.
9. Imhof A, Kratzner W, Boehm B, et al. Prevalence of non-alcoholic fatty liver and characteristics in overweight adolescents in the general population. *Eur J Epidemiol*. 2007;22(12):889-97.
10. Eckel RH, Grundy SM, Zimmet PZ. The metabolic syndrome. *Lancet*. 2005;365(9468):1415-28.
11. Madaj P, Budoff MJ. Risk stratification of non-contrast CT beyond the coronary calcium scan. *J Cardiovasc Comput Tomogr*. 2012;6(5):301-7.
12. Bastos M, Lee EY, Strauss KJ, Zurakowski D, Tracy DA, Boisselle PM. Motion artifact on high-resolution CT images of pediatric patients: comparison of volumetric and axial CT methods. *AJR American journal of roentgenology*. 2009;193(5):1414-8.
13. Yanagawa M, Tomiyama N, Sumikawa H, et al. Thin-section CT of lung without ECG gating: 64-detector row CT can markedly reduce cardiac motion artifact which can simulate lung lesions. *Eur J Radiol*. 2009;69(1):102-7.
14. Ko SF, Hsieh MJ, Chen MC, et al. Effects of heart rate on motion artifacts of the aorta on non-ECG-assisted 0.5-sec thoracic MDCT. *AJR American journal of roentgenology*. 2005;184(4):1225-30.
15. Fukuda A, Lin PJ, Matsubara K, Miyati T. Measurement of gantry rotation time in modern ct. *J Appl Clin Med Phys*. 2014;15(1):4517.
16. Bertheau RC, Bamberg F, Lochner E, et al. Whole-Body MR Imaging Including Angiography: Predicting Recurrent Events in Diabetics. *European radiology*. 2016;26(5):1420-30.
17. Sverzellati N, Arcadi T, Salvolini L, et al. Under-reporting of cardiovascular findings on chest CT. *La Radiologia medica*. 2016;121(3):190-9.

18. Erbel R, Mohlenkamp S, Moebus S, et al. Coronary risk stratification, discrimination, and reclassification improvement based on quantification of subclinical coronary atherosclerosis: the Heinz Nixdorf Recall study. *Journal of the American College of Cardiology*. 2010;56(17):1397-406.
19. Yeboah J, McClelland RL, Polonsky TS, et al. Comparison of novel risk markers for improvement in cardiovascular risk assessment in intermediate-risk individuals. *JAMA*. 2012;308(8):788-95.
20. Detrano R, Guerci AD, Carr JJ, et al. Coronary calcium as a predictor of coronary events in four racial or ethnic groups. *The New England journal of medicine*. 2008;358(13):1336-45.
21. Baber U, Mehran R, Sartori S, et al. Prevalence, impact, and predictive value of detecting subclinical coronary and carotid atherosclerosis in asymptomatic adults: the BioImage study. *Journal of the American College of Cardiology*. 2015;65(11):1065-74.
22. Budoff MJ, Young R, Burke G, et al. Ten-year association of coronary artery calcium with atherosclerotic cardiovascular disease (ASCVD) events: the multi-ethnic study of atherosclerosis (MESA). *Eur Heart J*. 2018;39(25):2401-8.
23. Perk J, De Backer G, Gohlke H, et al. European Guidelines on cardiovascular disease prevention in clinical practice (version 2012): The Fifth Joint Task Force of the European Society of Cardiology and Other Societies on Cardiovascular Disease Prevention in Clinical Practice (constituted by representatives of nine societies and by invited experts). *Atherosclerosis*. 2012;223(1):1-68.
24. Piepoli MF, Hoes AW, Agewall S, et al. 2016 European Guidelines on cardiovascular disease prevention in clinical practice: The Sixth Joint Task Force of the European Society of Cardiology and Other Societies on Cardiovascular Disease Prevention in Clinical Practice (constituted by representatives of 10 societies and by invited experts) Developed with the special contribution of the European Association for Cardiovascular Prevention & Rehabilitation (EACPR). *European heart journal*. 2016;37(29):2315-81.
25. Greenland P, Alpert JS, Beller GA, et al. 2010 ACCF/AHA guideline for assessment of cardiovascular risk in asymptomatic adults: executive summary: a report of the American College of Cardiology Foundation/American Heart Association Task Force on Practice Guidelines. *Circulation*. 2010;122(25):2748-64.
26. Taylor AJ, Cerqueira M, Hodgson JM, et al. ACCF/SCCT/ACR/AHA/ASE/ASNC/NASCI/SCAI/SCMR 2010 Appropriate Use Criteria for Cardiac Computed Tomography. A Report of the American College of Cardiology Foundation Appropriate Use Criteria Task Force, the Society of Cardiovascular Computed Tomography, the American College of Radiology, the American Heart Association, the American Society of Echocardiography, the American Society of Nuclear Cardiology, the North American Society for Cardiovascular Imaging, the Society for Cardiovascular Angiography and Interventions, and the Society for Cardiovascular Magnetic Resonance. *J Cardiovasc Comput Tomogr*. 2010;4(6):407 e1-33.
27. Brown SJ, Hayball MP, Coulden RA. Impact of motion artefact on the measurement of coronary calcium score. *Br J Radiol*. 2000;73(873):956-62.
28. Wu MT, Yang P, Huang YL, et al. Coronary arterial calcification on low-dose ungated MDCT for lung cancer screening: concordance study with dedicated cardiac CT. *AJR American journal of roentgenology*. 2008;190(4):923-8.
29. Kim SM, Chung MJ, Lee KS, Choe YH, Yi CA, Choe BK. Coronary calcium screening using low-dose lung cancer screening: effectiveness of MDCT with retrospective reconstruction. *AJR Am J Roentgenol*. 2008;190(4):917-22.
30. Htwe Y, Cham MD, Henschke CI, et al. Coronary artery calcification on low-dose computed tomography: comparison of Agatston and Ordinal Scores. *Clin Imaging*. 2015;39(5):799-802.
31. Blair KJ, Allison MA, Morgan C, et al. Comparison of ordinal versus Agatston coronary calcification scoring for cardiovascular disease mortality in community-living individuals. *Int J Cardiovasc Imaging*. 2014;30(4):813-8.

32. Shemesh J, Henschke CI, Shaham D, et al. Ordinal scoring of coronary artery calcifications on low-dose CT scans of the chest is predictive of death from cardiovascular disease. *Radiology*. 2010;257(2):541-8.
33. Mets OM, Vliegenthart R, Gondrie MJ, et al. Lung cancer screening CT-based prediction of cardiovascular events. *JACC Cardiovasc Imaging*. 2013;6(8):899-907.
34. Williams MC, Murchison JT, Edwards LD, et al. Coronary artery calcification is increased in patients with COPD and associated with increased morbidity and mortality. *Thorax*. 2014;69(8):718-23.
35. Chiles C, Duan F, Gladish GW, et al. Association of Coronary Artery Calcification and Mortality in the National Lung Screening Trial: A Comparison of Three Scoring Methods. *Radiology*. 2015;276(1):82-90.
36. Hughes-Austin JM, Dominguez A, 3rd, Allison MA, et al. Relationship of Coronary Calcium on Standard Chest CT Scans With Mortality. *JACC Cardiovasc Imaging*. 2016;9(2):152-9.
37. Shao L, Yan AT, Lebovic G, Wong HH, Kirpalani A, Deva DP. Prognostic value of visually detected coronary artery calcification on unenhanced non-gated thoracic computed tomography for prediction of non-fatal myocardial infarction and all-cause mortality. *J Cardiovasc Comput Tomogr*. 2017;11(3):196-202.
38. Gonzalez G, Washko GR, Estepar RS. Automated Agatston Score Computation in a Large Dataset of Non Ecg-Gated Chest Computed Tomography. *Proc IEEE Int Symp Biomed Imaging*. 2016;2016:53-7.
39. Hecht HS, Cronin P, Blaha MJ, et al. 2016 SCCT/STR guidelines for coronary artery calcium scoring of noncontrast noncardiac chest CT scans: A report of the Society of Cardiovascular Computed Tomography and Society of Thoracic Radiology. *Journal of thoracic imaging*. 2017;32(5):W54-W66.
40. Jairam PM, Gondrie MJ, Grobbee DE, et al. Incidental imaging findings from routine chest CT used to identify subjects at high risk of future cardiovascular events. *Radiology*. 2014;272(3):700-8.
41. Mahabadi AA, Lehmann N, Mohlenkamp S, et al. Noncoronary Measures Enhance the Predictive Value of Cardiac CT Above Traditional Risk Factors and CAC Score in the General Population. *JACC Cardiovascular imaging*. 2016;9(10):1177-85.
42. Kim J, Budoff MJ, Nasir K, et al. Thoracic aortic calcium, cardiovascular disease events, and all-cause mortality in asymptomatic individuals with zero coronary calcium: The Multi-Ethnic Study of Atherosclerosis (MESA). *Atherosclerosis*. 2017;257:1-8.
43. Hoffmann U, Massaro JM, D'Agostino RB, Sr., Kathiresan S, Fox CS, O'Donnell CJ. Cardiovascular Event Prediction and Risk Reclassification by Coronary, Aortic, and Valvular Calcification in the Framingham Heart Study. *J Am Heart Assoc*. 2016;5(2).
44. Liu F, Coursey CA, Grahame-Clarke C, et al. Aortic valve calcification as an incidental finding at CT of the elderly: severity and location as predictors of aortic stenosis. *AJR Am J Roentgenol*. 2006;186(2):342-9.
45. O'Brien KD. Pathogenesis of calcific aortic valve disease: a disease process comes of age (and a good deal more). *Arterioscler Thromb Vasc Biol*. 2006;26(8):1721-8.
46. Mathieu P, Despres JP, Pibarot P. The 'valvulo-metabolic' risk in calcific aortic valve disease. *Can J Cardiol*. 2007;23 Suppl B:32B-9B.
47. Mahabadi AA, Bamberg F, Toepker M, et al. Association of aortic valve calcification to the presence, extent, and composition of coronary artery plaque burden: from the Rule Out Myocardial Infarction using Computer Assisted Tomography (ROMICAT) trial. *Am Heart J*. 2009;158(4):562-8.
48. Revilla-Orodea A, Toro-Gil JA, Sevilla T, et al. Coronary artery and aortic valve calcification evaluated with cardiac computed tomography in patients with chest pain: Prognostic value in clinical practice. *Int J Cardiol*. 2016;219:247-50.
49. Willemink MJ, Takx RA, Isgum I, et al. Prognostic value of heart valve calcifications for cardiovascular events in a lung cancer screening population. *Int J Cardiovasc Imaging*. 2015;31(6):1243-9.

50. Gondrie MJ, van der Graaf Y, Jacobs PC, Oen AL, Mali WP, Group PS. The association of incidentally detected heart valve calcification with future cardiovascular events. *European radiology*. 2011;21(5):963-73.
51. Abramowitz Y, Jilaihawi H, Chakravarty T, Mack MJ, Makkar RR. Mitral Annulus Calcification. *Journal of the American College of Cardiology*. 2015;66(17):1934-41.
52. Fox CS, Vasan RS, Parise H, et al. Mitral annular calcification predicts cardiovascular morbidity and mortality: the Framingham Heart Study. *Circulation*. 2003;107(11):1492-6.
53. Holtz JE, Upadhyaya DS, Cohen BE, Na B, Schiller NB, Whooley MA. Mitral annular calcium, inducible myocardial ischemia, and cardiovascular events in outpatients with coronary heart disease (from the Heart and Soul Study). *Am J Cardiol*. 2012;109(8):1092-6.
54. Mahnken AH, Muhlenbruch G, Das M, et al. MDCT detection of mitral valve calcification: prevalence and clinical relevance compared with echocardiography. *AJR Am J Roentgenol*. 2007;188(5):1264-9.
55. Kohsaka S, Jin Z, Rundek T, et al. Impact of mitral annular calcification on cardiovascular events in a multiethnic community: the Northern Manhattan Study. *JACC Cardiovasc Imaging*. 2008;1(5):617-23.
56. Potpara TS, Vasiljevic ZM, Vujisic-Tesic BD, et al. Mitral annular calcification predicts cardiovascular morbidity and mortality in middle-aged patients with atrial fibrillation: the Belgrade Atrial Fibrillation Study. *Chest*. 2011;140(4):902-10.
57. Aijaz B, Ammar KA, Lopez-Jimenez F, Redfield MM, Jacobsen SJ, Rodeheffer RJ. Abnormal cardiac structure and function in the metabolic syndrome: a population-based study. *Mayo Clin Proc*. 2008;83(12):1350-7.
58. Ladeiras-Lopes R, Moreira HT, Bettencourt N, et al. Metabolic Syndrome Is Associated With Impaired Diastolic Function Independently of MRI-Derived Myocardial Extracellular Volume: The MESA Study. *Diabetes*. 2018;67(5):1007-12.
59. Schlett CL, Kwait DC, Mahabadi AA, et al. Simple area-based measurement for multidetector computed tomography to predict left ventricular size. *European radiology*. 2010;20(7):1590-6.
60. Mahabadi AA, Truong QA, Schlett CL, et al. Axial area and anteroposterior diameter as estimates of left atrial size using computed tomography of the chest: comparison with 3-dimensional volume. *J Cardiovasc Comput Tomogr*. 2010;4(1):49-54.
61. Truong QA, Bamberg F, Mahabadi AA, et al. Left atrial volume and index by multi-detector computed tomography: comprehensive analysis from predictors of enlargement to predictive value for acute coronary syndrome (ROMICAT study). *Int J Cardiol*. 2011;146(2):171-6.
62. Mahabadi AA, Geisel MH, Lehmann N, et al. Association of computed tomography-derived left atrial size with major cardiovascular events in the general population: the Heinz Nixdorf Recall Study. *Int J Cardiol*. 2014;174(2):318-23.
63. Jivraj K, Bedayat A, Sung YK, et al. Left Atrium Maximal Axial Cross-Sectional Area is a Specific Computed Tomographic Imaging Biomarker of World Health Organization Group 2 Pulmonary Hypertension. *Journal of thoracic imaging*. 2017;32(2):121-6.
64. Murphy DJ, Lavelle LP, Gibney B, O'Donohoe RL, Remy-Jardin M, Dodd JD. Diagnostic accuracy of standard axial 64-slice chest CT compared to cardiac MRI for the detection of cardiomyopathies. *Br J Radiol*. 2016;89(1059):20150810.
65. Bhatt SP, Vegas-Sanchez-Ferrero G, Rahaghi FN, et al. Cardiac Morphometry on Computed Tomography and Exacerbation Reduction with beta-Blocker Therapy in Chronic Obstructive Pulmonary Disease. *Am J Respir Crit Care Med*. 2017;196(11):1484-8.
66. Manno C, Campobasso N, Nardecchia A, et al. Relationship of para- and perirenal fat and epicardial fat with metabolic parameters in overweight and obese subjects. *Eat Weight Disord*. 2018.

67. Hedgire S, Baliyan V, Zucker EJ, et al. Perivascular Epicardial Fat Stranding at Coronary CT Angiography: A Marker of Acute Plaque Rupture and Spontaneous Coronary Artery Dissection. *Radiology*. 2018;287(3):808-15.
68. Hartiala O, Magnussen CG, Bucci M, et al. Coronary heart disease risk factors, coronary artery calcification and epicardial fat volume in the Young Finns Study. *Eur Heart J Cardiovasc Imaging*. 2015;16(11):1256-63.
69. Antonopoulos AS, Sanna F, Sabharwal N, et al. Detecting human coronary inflammation by imaging perivascular fat. *Sci Transl Med*. 2017;9(398).
70. Nakamoto T. Sleep-Disordered Breathing-a Real Therapeutic Target for Hypertension, Pulmonary Hypertension, Ischemic Heart Disease, and Chronic Heart Failure? *J Nippon Med Sch*. 2018;85(2):70-7.
71. Kim AM, Keenan BT, Jackson N, et al. Tongue fat and its relationship to obstructive sleep apnea. *Sleep*. 2014;37(10):1639-48.
72. Mazzuca E, Battaglia S, Marrone O, et al. Gender-specific anthropometric markers of adiposity, metabolic syndrome and visceral adiposity index (VAI) in patients with obstructive sleep apnea. *J Sleep Res*. 2014;23(1):13-21.
73. Leng Y, McEvoy CT, Allen IE, Yaffe K. Association of Sleep-Disordered Breathing With Cognitive Function and Risk of Cognitive Impairment: A Systematic Review and Meta-analysis. *JAMA Neurol*. 2017;74(10):1237-45.
74. Dobrowolski P, Florcza E, Klisiewicz A, et al. Pulmonary artery dilation indicates severe obstructive sleep apnea in patients with resistant hypertension: the Resist-POL Study. *Pol Arch Med Wewn*. 2016;126(4):222-9.
75. Corson N, Armato SG, Labby ZE, Straus C, Starkey A, Gomberg-Maitland M. CT-based pulmonary artery measurements for the assessment of pulmonary hypertension. *Academic radiology*. 2014;21(4):523-30.
76. Truong QA, Massaro JM, Rogers IS, et al. Reference values for normal pulmonary artery dimensions by noncontrast cardiac computed tomography: the Framingham Heart Study. *Circ Cardiovasc Imaging*. 2012;5(1):147-54.
77. Renapurkar RD, Shrikanthan S, Heresi GA, Lau CT, Gopalan D. Imaging in Chronic Thromboembolic Pulmonary Hypertension. *Journal of thoracic imaging*. 2017;32(2):71-88.
78. Tabari A, Lo Gullo R, Murugan V, Otrakji A, Digumarthy S, Kalra M. Recent Advances in Computed Tomographic Technology: Cardiopulmonary Imaging Applications. *Journal of thoracic imaging*. 2017;32(2):89-100.
79. Padole A, Singh S, Ackman JB, et al. Submillisievert chest CT with filtered back projection and iterative reconstruction techniques. *AJR American journal of roentgenology*. 2014;203(4):772-81.
80. Shemesh J. Coronary artery calcification in clinical practice: what we have learned and why should it routinely be reported on chest CT? *Ann Transl Med*. 2016;4(8):159.
81. Kockelkoren R, Jairam PM, Murchison JT, et al. Validation of an imaging based cardiovascular risk score in a Scottish population. *Eur J Radiol*. 2018;98:143-9.

Legends

Legend Figure 1: Data from Wu et al (28) in a study comparing Agatston Calcium Scores on non-cardiac gated, non-contrast low dose CT (LDCT) performed for lung cancer screening to standard cardiac gated, non-contrast computed tomography (NCCT) in 513 consecutive cases. This shows excellent correlation between these two ways to quantify Agatston coronary artery calcification scores ($R^2=0.95$). They found a systematic under quantification of CAC using LDCT (y intercept = -12.1). Thus, any coronary artery calcification found at LDCT is worthy of quantification. This can be performed either by ordinal scoring or using post processing to obtain the non-cardiac gated LDCT Agatston score. (Scatter plot of the raw data made expressly for this article by Ming-Ting Wu, M.D.)

Legend Figure 2: Non gated, non-contrast computed tomography of the chest with globular calcification of an atherosclerotic plaque at the origin of the left anterior descending coronary artery (arrow head).

Legend Figure 3: Non-gated, non-contrast computed tomography of the chest coned down to the heart (A) axial and (B) short axis reconstruction showing a fibrofatty subendocardial scar (arrows) in the left ventricular septum, inferior and inferolateral walls from an old myocardial infarction in the right coronary artery vascular territory. Note the presence of hepatic steatosis as well (A) with a liver density of 35 Hounsfield units (ROI -Region of interest).

Legend Figure 4: 45 year old Caucasian male with (A) borderline evidence for low iodine organification in the thyroid with a thyroid density of 64 (Normal range 80-120 HU) (B) non gated Agatston score of 2 is at least in the 79th percentile for age and sex. There was hepatic steatosis as well (C) with a liver density of 42.9 HU. The

paraspinal muscle density was low measuring 33.8 HU at the T12 level (Normal range 5-60HU, from unpublished data (Tsuchiya et al, submitted)). This constellation of findings is the imaging equivalent of the clinically defined Metabolic Syndrome and suggests both glucose intolerance and an increase in overall inflammatory cytokines due to the low paraspinal muscle density.

Legend Figure 5: Pulmonary trunk measured at the largest part of the right main pulmonary artery is 4.0 cm (white line). This is abnormal and is suggestive of the possibility of pulmonary hypertension/pulmonary arterial hypertension. In an obese individual a common cause is sleep disordered breathing (sleep apnea) which can be treated with a night time Continuous Positive Airway Pressure (CPAP) mask.

Legend Supplemental Figure 1: Automatic segmentation of the left and right ventricular cavities from non contrast non cardiac gated chest CT exams using the method of Bhatt et al (65), (A) axial chest CT with the estimated left ventricle cavity in light red and the estimated left ventricular wall in dark red, with the estimated right ventricle in blue, (B) sagittal non contrast CT showing the estimated left ventricle in red and the estimated right ventricle in blue. (C) coronal chest CT showing the estimated left ventricle in red and the estimated right ventricle in blue, (D) Entire volume of left ventricle in red and right ventricle in blue.

Legend Table 1: Importance of coronary artery calcification found on non-cardiac gated chest computed tomography in patients that smoke cigarettes (table modified from Shemesh et al) (80) Practical comments for chest radiologists showing that the larger ordinal coronary artery calcium score is associated with an increased risk of Major Adverse Cardiac Events. (This table is modified from Shemesh et al (80)) Abbreviations: CAC- coronary artery calcium score; Visual Score (Likert Scale range from 0-12); CAD- coronary artery disease, PVD- peripheral vascular disease;

Legend Table 2: Imaging findings on non-contrast, non-cardiac gated Chest Computed tomography exams that are reflective of individual biology and the metabolic syndrome. (Abbreviations: n- number affected. N=total in study)

Legend Table 3: Imaging based cardiovascular risk biomarkers derived from a Caucasian population in Scotland (N= 2124) (81). This type of analytic approach to documenting vascular calcifications was first used by Jairam et al in 2014 (40).

Legend Table 4: Hazard Ratios for the most significant model parameters for determining cardiovascular risk from contrast enhanced, non-gated chest CT exams from the PROVIDI study (N=10,410) (40).

Legend Table 5: Multivariable analysis of clinical and imaging based cardiovascular risk biomarkers derived from 3,630 subjects enrolled in the prospectively acquired Hienz-Nixdorff Recall Study. (41) and their adjusted Hazard Ratios for the interval development of major adverse cardiac events (MACE). (Abbreviations: FR- Framingham Risk Score, CAC- Coronary artery Agatston Score,)

Legend Table S1: Multi-Ethnic Study of Atherosclerosis (MESA) results from Budoff et al(22) modified from Table 2 in the original publication, showing the ten year event rate of major adverse cardiac events based simply off of the gated CT chest coronary artery Agatston calcium scores. These event rates are not adjusted for any clinical risk factors. These data show the effects of CAC transcend age related changes; in that more CAC is worse than simply being old. The Chinese and Caucasian were less affected by CAC than African-Americans and Hispanics.

Legend Tables S2 and S3: Kockelkoren (81) Scottish heart study risk 10 year estimated risk model (Table S2) and the equation used to derive the 5 year risk score (Table S3)

Figures

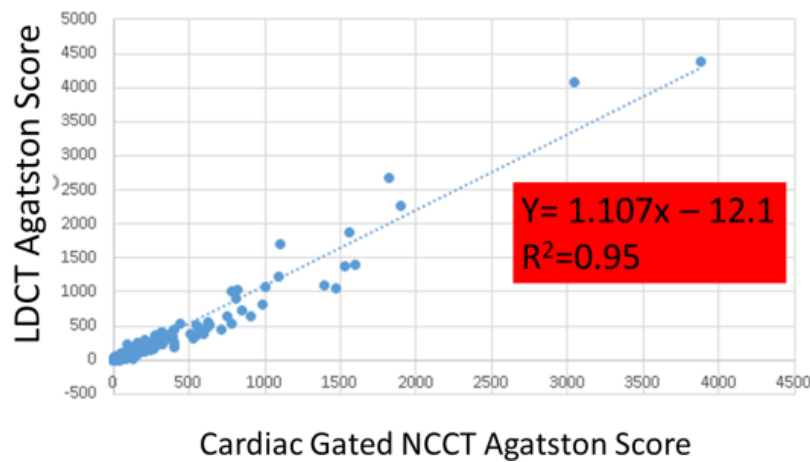
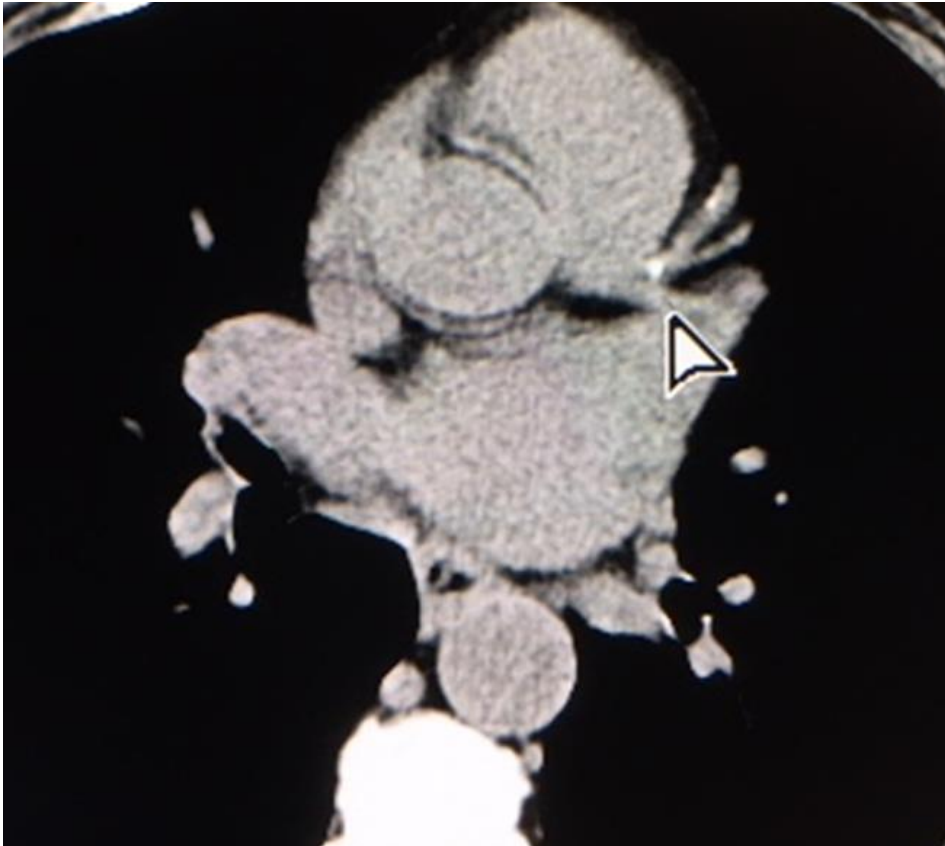
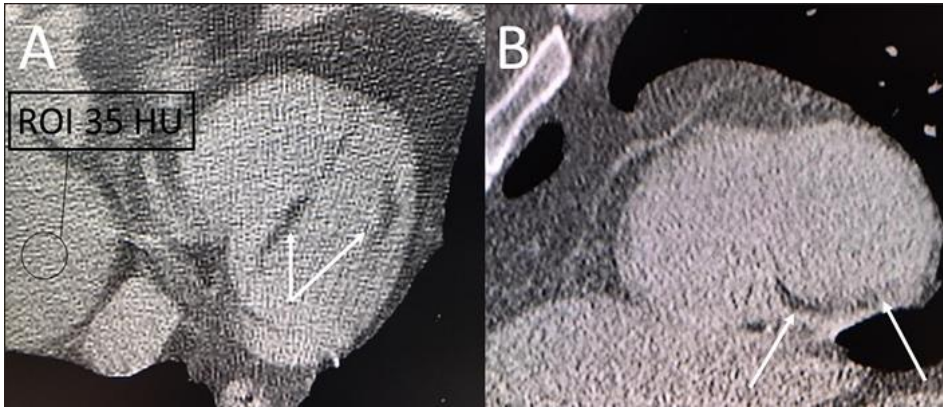


Figure 1: Data from Wu et al (28) in a study comparing Agatston Calcium Scores on non-cardiac gated, non-contrast low dose CT (LDCT) performed for lung cancer screening to standard cardiac gated, non-contrast computed tomography (NCCT) in 483 cases. This shows excellent correlation between these two ways to quantify Agatston coronary artery calcification scores ($R^2=0.95$). They found a systematic under quantification of CAC using LDCT (y intercept = -12.1). Thus, any coronary artery calcification found at LDCT is worthy of quantification. This can be performed either by ordinal scoring or, as in this study, using post processing to obtain the non-cardiac gated LDCT Agatston score. (Scatter plot of the raw data from (28) made expressly for this article by Ming-Ting Wu, M.D.)

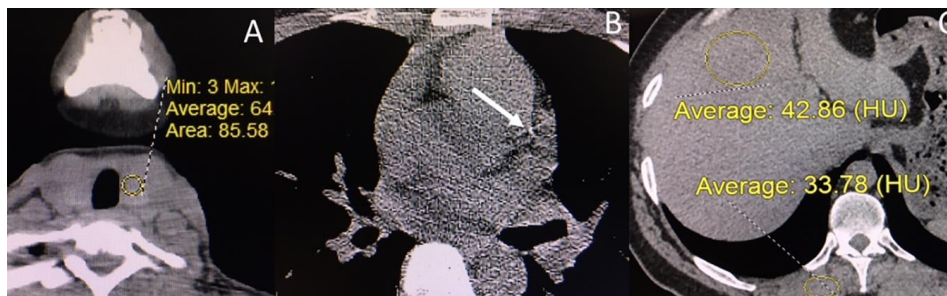
Figure 2



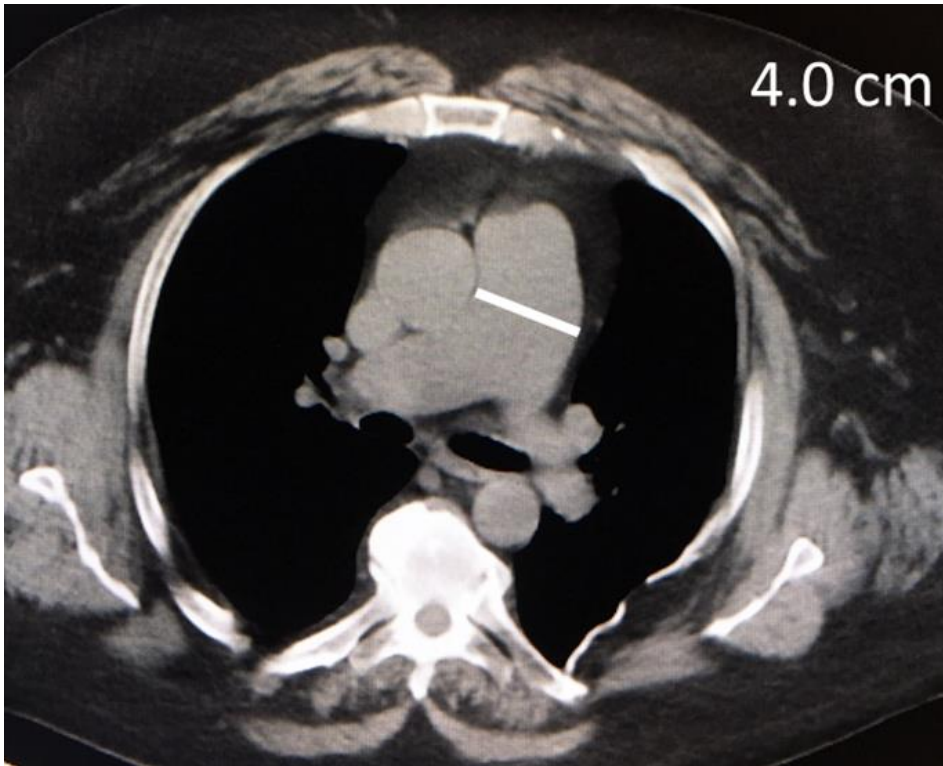
Legend Figure 2: Non gated, non-contrast computed tomography of the chest with globular calcification of an atherosclerotic plaque at the origin of the left anterior descending coronary artery (arrow head).



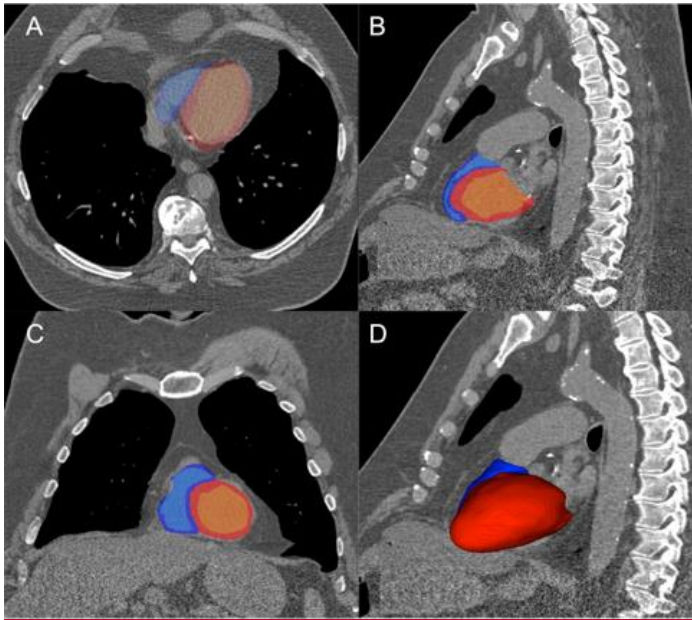
Legend Figure 3: Non gated, non-contrast computed tomography of the chest coned down to the heart (A) axial and (B) short axis reconstruction showing a fibrofatty subendocardial scar (arrows) in the left ventricular septum, inferior and inferolateral walls from an old myocardial infarction in the right coronary artery vascular territory. Note the presence of hepatic steatosis as well (A) with a liver density of 35 Hounsfield units (ROI -Region of interest).



Legend Figure 4: 45 year old Caucasian male with (A) borderline evidence for low iodine organification in the thyroid with a thyroid density of 64 (Normal range 80-120 HU) (B) non gated Agatston score of 2 is at least in the 79th percentile for age and sex. There was hepatic steatosis as well (C) with a liver density of 42.9 HU. The paraspinal muscle density was low measuring 33.8 HU at the T12 level (Normal range 5-60HU, from unpublished data (Tsuchiya et al, submitted)). This constellation of findings is the imaging equivalent of the clinically defined Metabolic Syndrome and suggests both glucose intolerance and an increase in overall inflammatory cytokines due to the low paraspinal muscle density.



Legend Figure 5: Pulmonary trunk measured at the largest part of the right main pulmonary artery is 4.0 cm (white line). This is abnormal and is suggestive of the possibility of pulmonary hypertension/pulmonary arterial hypertension. In an obese individual a common cause is sleep disordered breathing (sleep apnea) which can be treated with a night time Continuous Positive Airway Pressure (CPAP) mask.



Legend Supplemental Figure 1: Automatic segmentation of the left and right ventricular cavities from non contrast non cardiac gated chest CT exams using the method of Bhatt et al (65), (A) axial chest CT with the estimated left ventricle cavity in light red and the estimated left ventricular wall in dark red, with the estimated right ventricle in blue, (B) sagittal non contrast CT showing the estimated left ventricle in red and the estimated right ventricle in blue, (C) coronal chest CT showing the estimated left ventricle in red and the estimated right ventricle in blue, (D) Entire volume of left ventricle in red and right ventricle in blue.

Formatted: Font: Bold

Table 1:

	Agatston Score	Visual Score (0-12)	Prognosis	Recommendation	Comment
No CAC	0	0	More favorable prognosis for CV events;	The presence of chronic obstructive CAD is very unlikely, life style changes	Might be false negative since small calcific lesions are missed (Agatston score <10): the visual score is less sensitive in subjects with low CAC burden
Mild CAC	1-100	1-4	Mildly increased risk for CV event	Consider further coronary evaluation and primary preventive treatment according to the patient global risk, life style changes should be more emphasized.	
Moderate CAC	101-400	5-7	Mildly increased risk of CV event	Consider further coronary evaluation and primary preventive treatment according to the patient global risk and clinical manifestations; in patients with Framingham risk intermediate and above ($\geq 10\%$ in 10 years) statin should be considered.	
Severe CAC	>400	8-12	Significantly increases the CV risk and total mortality	In asymptomatic subjects, consider further coronary evaluation by stress ECG, stress echo or SPECT imaging to R/O obstructive CAD; statin therapy should be highly considered.	Mostly prevalent in old patients and in those with clinical CAD, PVD and renal failure

Table 1: Importance of coronary artery calcification found on non-cardiac gated chest computed tomography in patients that smoke cigarettes (table modified from Shemesh et al) (80) Practical comments for chest radiologists showing that the larger ordinal coronary artery calcium score is associated with an increased risk of Major Adverse Cardiac Events. (This table is modified from Shemesh et al (80)) Abbreviations: CAC- coronary artery calcium score; Visual Score (Likert Scale range from 0-12); CAD- coronary artery disease, PVD- peripheral vascular disease;

Table 2

Non contrast, Chest CT finding	Index cases(n)/ Normal Values (N) [n/N]	Abnormal Value [n/N]	Unadjusted Hazard Ratio For MACE or Death (95% C.I) _p value_	Adjusted Hazard Ratio (95% CI) _p value_	Reference
Heart					
Transverse diameter of heart					Leiner article
Left Atrial Index, mm ² /m ²	917 ±187 [3389/3630]	992 ± 214 [241/3630]	1.42 (1.27-1.59) _<0.0001_	1.18 (1.02- 1.37) _0.023_	Gated exam Mahabadi 2016
Left Ventricular Index, mm ² /m ²	2,146 ± 275 [3389/3630]	2,240 ± 305 [241/3630]	1.36 (1.21-1.52) _<0.0001_	1.08 (0.93- 1.25) _0.31_	Gated exam Mahabadi 2016
Epicardial Fat Volume, ml	92.7 ± 46.0 [3389/3630]	117.5 ± 55.6 [241/3630]	1.52 (1.38-1.68) _<0.0001_	1.18 (1.02- 1.34) _0.023_	Gated exam Mahabadi 2016 <0.0001

Non Gated Coronary artery Calcifications Ordinal Score					Chiles
Non Gated Coronary artery Calcifications Volume					Consensus statement
Non Gated Coronary artery Calcifications Agatston Score					Consensus statement
Ascending or Descending Aortic Calcification	Ca++ present 61.5% [2083/3630]	Ca++ present 77.2% [186/241]	2.08 (1.54-2.81) _0.0001_	1.14 (0.83- 1.57) _0.41_	Gated exam Mahabadi 2016 (<0.0001)
Aortic Valve Calcifications	Ca++ Present 10.3% [324/3,389]	Ca++ Present 19.9% [48/241]	2.34 (1.7-3.2) _0.0001_	1.03 (0.73- 1.44) _0.88_	Gated exam Mahabadi 2016
Ascending Aortic Diameter at Pul Art bifurcation	35.5 ± 4.0 [3389/3630]	37.1 ± 4.1 [241/3630]	1.44 (1.29-1.61) _0.0001_	1.02 (0.94- 1.06) _0.25_	Gated exam Mahabadi 2016
Descending Aortic Diameter (mm) at Pul Art bifurcation	26.5 ± 2.9 [3389/3630]	27.9 ± 2.7 [241/3630]	1.56 (1.39-1.76) _<0.0001_	0.94 (0.88- 1.03) _0.06_	Gated exam Mahabadi 2016
Mitral Valve Leaflet Calcium					Andreas H. Mahnken ^{1,2}
Mitral Valve Annulus Calcium	2.4% [76/3,389]	4.2% [10/241]	1.9 (1.01-3.58) _0.0001_	0.73 (0.38- 1.40) _0.34_	Gated exam Mahabadi 2016

Legend Table 2: Imaging findings on non-contrast, non-cardiac gated Chest Computed tomography exams that are reflective of individual biology and the metabolic syndrome. (Abbreviations: n- number affected. N=total in study)

Table 3

NCCT imaging Finding	Absent Score=0	Mild Score=1	Moderate Score=2	Severe Score=3
Left anterior descending coronary artery calcification	none	1 or 2 calcified plaques limited to 2 or fewer images	Greater than 2 focal plaques or calcification extending for more than 2 slices	Fully calcified coronary artery extending for more than 3 slices
Descending Thoracic Aorta Calcification	none	Less than or equal to 3 focal calcified plaques	4-5 focal calcified plaques or one plaque extending for 3 or more slices	More than 5 focal calcified plaques or 2 plaques extending beyond 3 slices
Mitral valve leaflet Calcification	none	One leaflet calcified	Two leaflets calcified	

Legend Table 3: Imaging based cardiovascular risk biomarkers derived from a Caucasian population in Scotland (N= 2124) (81). This type of analytic approach to documenting vascular calcifications was first used by Jairam et al in 2014 (40).

Table 4

Model feature	Hazard Ratio	P value
Male	1.41	<0.001
Descending Aorta Calcification	1.45	<0.001
Mitral Valve Calcification	1.25	<0.001
LAD Calcification	1.11	<0.003
(Maximum Transverse Cardiovascular diameter in cm - 11cm) ²	1.03	<0.001
Age	1.03	<0.001

Legend Table 4: Hazard Ratios for the most significant model parameters for determining cardiovascular risk from contrast enhanced, non-gated chest CT exams from the PROVIDI study (N=10,410) (40).

Table 5

Model feature	Hazard Ratio Adjusted for FR score, CAC score and Multiple CT measures (95% C.I.)	P value
Left atrial index	1.21 (1.07-1.36)	0.002
Left ventricular index	1.15 (1.02-1.29)	0.02
Epicardial Fat Volume	1.14 (1.01-1.28)	0.04
<i>Presence of Thoracic Aortic Calcification</i>	1.14 (0.83-1.56)	0.43
<i>Diameter of Ascending aorta</i>	0.98 (0.84-1.15)	0.25

<i>Aortic Valve Calcification</i>	<i>1.01</i> <i>(0.72-1.40)</i>	<i>0.98</i>
<i>Diameter of the Descending thoracic Aorta</i>	<i>0.98</i> <i>(0.84-1.15)</i>	<i>0.84</i>
<i>Mitral Annulus Calcification</i>	<i>0.81</i> <i>(0.43-1.54)</i>	<i>0.81</i>

Legend Table 5: Multivariable analysis of clinical and imaging based cardiovascular risk biomarkers derived from 3,630 subjects enrolled in the prospectively acquired Hienz-Nixdorff Recall Study. (41) and their adjusted Hazard Ratios for the interval development of major adverse cardiac events (MACE). (Abbreviations: FR- Framingham Risk Score, CAC- Coronary artery Agatston Score,)

Table S1

	Ten year event rate	Ten year event rate	Ten year event rate	Ten year event rate
	CAC 0	CAC 1-100	CAC 101- 300	CAC 300+

Ages 75-85	5.6	14.3	18.1	24.7
African-American	3.9	7.7	14.7	24.5
Hispanic	3.1	10.3	19.1	21.7
Not On Lipid lowering meds(baseline)	2.7	7.7	13.4	19.9
Female	2.8	7.3	10.6	19.0
Male	3.0	8.0	14.4	18.2
Ages 55-64	3.1	6.5	8.6	16.7
On lipid lowering agents at baseline	2.8	7.4	12.9	16.5
Ages 45-54	1.7	3.8	15.4	16.2
Caucasian	2.4	7.3	10.8	16.2
Ages 65-74	4.2	8.3	11.8	15.0
Chinese	1.3	4.7	8.3	13.1

Legend Table S1: Multi-Ethnic Study of Atherosclerosis (MESA) results from Budoff et al(22) modified from Table 2 in the original publication, showing the ten year event rate of major adverse cardiac events based simply off of the gated CT chest coronary artery Agatston calcium scores. These event rates are not adjusted for any clinical risk factors. These data show the effects of CAC transcend age related changes; in that more CAC is worse than simply being old. The Chinese and Caucasian were less affected by CAC than African-Americans and Hispanics.

Supplementary Table S2:

Kockelkoren risk model (81)

Predicted vs Observed 10 year cardiovascular risk

Risk Group	10y Risk: Radiological risk score
Low risk group (<10% risk)	
No. of patients n (%)	200 (9)
Observed Kaplan-Meier risk (%)	9.8%
Intermediate risk group (10-20% risk)	
No. of patients n (%)	523 (25)
Observed Kaplan-Meier risk (%)	18.8%

High risk group (>20% risk)

No. of patients n (%) 1401 (66)

Observed Kaplan-Meier risk (%) 36.5%

* 10y observed CVD risk was obtained by extrapolating the cumulative baseline hazard function

Legend Tables S2 and S3: Kockelkoren(81) Scottish heart study risk 10 year estimated risk model(Table S2) and the equation used to derive the 5 year risk score (Table S3)

Supplementary Table S3**Model parameters (81)**

5-year cardiovascular disease event risk (%) = $[1 - 0.88^{\exp(A - 2.16)}] \times 100\%$

A = (0.027 x Age) + (0.34 if male gender) – (0.33 if CT-indication hematological malignancies) – (0.34 if CT-indication mediastinal abnormalities) – (0.27 if CT-indication suspicion pulmonary malignancy) + (0.034 if CT-indication suspicion pulmonary embolism) – (0.30 if other CT-indication) + (0.10 x score [LAD calc]) + (0.22 x score [MV calc]) + (0.37 x [DSC calc]) + (0.02 x [Cardiac diameter* - 11cm]²)

* Cardiac diameters below 11 cm get value “0”, from higher diameters subtract 11 and square the resulting value.

Legend Tables S2 and S3: Kockelkoren(81) Scottish heart study risk 10 year estimated risk model(Table S2) and the equation used to derive the 5 year risk score (Table S3)

**Non-Contrast Chest Computed Tomographic Imaging of Obesity and the Metabolic Syndrome (MetS): Part 1
Cardiovascular Findings**

Abstract

There are physiological consequences of overeating that can lead to increased morbidity and mortality. Purpose of this review article is to acquaint the reader with the current state of the art in the non-cardiac gated, non-contrast chest Computed Tomographic (NCCT) imaging biomarkers of the metabolic syndrome (MetS) and their prognostic significance found in the lower neck and chest. NCCT Imaging biomarkers, associated with MetS in the chest include premature coronary artery calcification, acceleration of large vessel arterial and valvular calcifications associated with atherosclerosis, and pulmonary arterial enlargement from pulmonary hypertension associated with sleep apnea. These easily identified imaging biomarkers have prognostic implications for Major Adverse Cardiac Events (MACE). These NCCT chest-imaging biomarkers are likely targets for artificial intelligence algorithms to harvest for longitudinal assessment of their individual and multifactorial contributions to chronic disease, MACE and mortality. Early recognition and treatment of these common disorders may help improve patient outcomes and quality of life while decreasing medical costs.

Key words (Mesh Terms): Humans, Biomarkers, Prognosis, Metabolic Syndrome, Tomography, X-ray computed, Calcium Scoring, Atherosclerosis, Sleep apnea syndrome, Pulmonary Hypertension, Thorax

Abbreviations:

AVC	Aortic Valve leaflet Calcification
CAC	Coronary Artery Calcification
CT	Computed Tomography
DSC Ca++	DeSCending aorta Calcium value
FR	Framingham Risk Score
HR	Hazard Ratio
HU	Hounsfield unit
LA	Left Atrium
LAD Ca++	Left Anterior Descending coronary artery Calcium value,
LA-MACSA	Left atrial maximal cross-sectional area (mm ²)
LV	Left Ventricle
MAC	Mitral valve Annulus Calcification
MACE	Major adverse cardiovascular event
MV CA++	Mitral Valve leaflet Calcification
MetS	Metabolic Syndrome (a.k.a. Syndrome X)
NCCT	Non contrast Computed Tomography
NG-NCCT	Non cardiac Gated, Non-Contrast chest Computed Tomography
OSA	Obstructive Sleep Apnea
PH	Pulmonary Hypertension
mPAP	mean Pulmonary Artery Pressure
RV	Right Ventricle
TAC	Thoracic Aortic Calcification

Introduction

Cardiovascular disease (CVD) is the number one cause of mortality with an estimated 17.9 million deaths worldwide in 2015 (1). This represents an increasing problem for public health in both developed and developing countries (1). The metabolic syndrome (MetS) is a complex disorder of metabolism which results in an increased risk for CVD and Type 2 diabetes (2). It is comprised of a cluster of risk factors including elevated blood pressure, dyslipidaemia (lowered high-density lipoprotein (HDL) cholesterol and elevated triglycerides), elevated fasting glucose and central obesity (2). The American Heart Association/ ATP III definition of MetS is dependent on three of the five risk factors being present (2):

enlarged waist circumference with population-specific and country-specific criteria; triglycerides ≥ 150 mg/dL, HDL-c < 40 mg/dL in men and < 50 mg/dL in women, systolic blood pressure ≥ 130 mm Hg or diastolic blood pressure ≥ 85 mm Hg and fasting glucose > 100 mg/dL, with the inclusion of patients taking medication to manage hypertriglyceridemia, low HDL-c, hypertension and hyperglycemia.(2).

All parts of the body are affected by MetS. Recently, Bizino et al, reviewed the role of MRI for the study of MetS in the entire body.(3) Work on the gut-brain axis also shows that there is bidirectional signalling between the two organs and that the metabolome in the gut, which is influenced by a high fat/refined sugar diet, has critical roles in host metabolism, the brain reward system and behavior. (4) Put into more mundane terms, “the comfort foods of sugar and fat taste good and the brain wants more than the body needs.” This trend for overindulgence in food and sugar filled, and/or alcoholic drinks, spells trouble for the future of medical care expenditures in the developed world.

The underlying pathophysiology of MetS is related to the induction of low-grade systemic inflammation via increased levels of inflammatory cytokines (e.g. IL-6, IL-1 and TNF- α), adipokines and leptin, which originate from adipocytes or macrophages in the fat tissue. (5) This inflammatory process contributes to atherosclerosis, metabolic dysfunction and results in MetS. This increase in inflammation also effects the lung function by activation of

fibroblasts, endothelial cells of the lung vessels, airway epithelial and smooth muscle cells. This helps to explain why asthma is more severe in obese individuals. (5) Also, insulin resistance increases in asthmatics as insulin alters airway function and structure. (5) Obesity is thus associated with severe asthma induced by low-grade systemic inflammation and insulin resistance, which implies that strategies to treat insulin resistance, obesity and systemic inflammation could work also for asthma. (5, 6)

The prevalence of obesity in adults, defined as BMI $>25.0 \text{ kg/m}^2$, has increased worldwide from 1980 to 2013: in women from 29.8 to 38.0 % and in men from 28.8 to 36.9 %. (7) This problem is not limited to the adult population, as childhood obesity has also become an increasing problem with important future consequences for public health expenditures, morbidity and mortality. (7) Reasons for this increase are high caloric diet, changes of diet composition, changes in microbiome of gut, changes in behaviour and lack of physical exercise. (7) In the developing countries, obesity increased from 8.4 to 13.4 in girls and from 8.1 to 12.9% in boys, while the proportion of obesity in the developed countries meanwhile is 22.6% in girls and 23.8 in boys. (7) As a consequence, cardiovascular dysfunction, diabetes or fatty liver disease with possible progression to end stage liver disease are apparent at an early age. (7-9) As the developed world ages, the health effects of obesity (MetS, Type 2 diabetes, cardiovascular disease and osteoarthritis of the spine, knees and hips) will demand an even larger portion of future public health expenditures.

The purpose of this review is to acquaint radiologists with the current state of the art in the non-cardiac gated, non-contrast chest computed tomography (NG-NCCT) cardiovascular imaging biomarkers found patients with obesity and the metabolic syndrome (MetS) and their prognostic significance. Our aim is to help identify those persons at risk using the metrics from these imaging biomarkers and to then recommend lifestyle interventions (weight reduction, increased physical activity and nutritional intervention) and a modification of medical management or surgery to improve patient outcomes. (10)

Heart and great vessels

The progression of cardiac and vascular disease takes place over decades and is for the most part asymptomatic. Thus, without testing the patient is not aware of the degree of his/her atherosclerotic burden. NG-NCCT can detect and quantify early heart disease and serve as a prognostic marker, particularly in patients with MetS. Madaj and Budoff published a nice summary of the risk stratification that NCCT can provide.(11) Given the limited soft-tissue contrast of non-enhanced CT, most prognostic markers are based on the quantification of calcification - either as part of vascular arteriosclerosis or valve leaflet calcification. While all cardiac structures are affected by cardiac motion, there is increasing evidence that, with newer hardware, and faster gantry rotation times, low-dose NG-NCCT cardiac motion is less of a problem for calcification and myocardial scar assessment/quantification (**Figures 1-4**).(12-15) Furthermore, arteriosclerosis is a systemic disease and although the association is stronger between atherosclerotic alteration and development of further events in the same organ segment (16), assessment of one vascular bed may serve as a proxy for an overall risk marker. However, a significant portion of potentially clinically significant cardiovascular findings are currently not mentioned in the written reports, particularly by junior radiologists.(17)

Coronary artery Calcification

The most important non-acute finding on NCCT predictive of future major adverse cardiac events is coronary artery calcification (CAC) (**Figures 2 and 4**). Broad evidence exists regarding the prognostic value of coronary artery calcification (CAC) for cardiovascular events (18-22). More importantly, the use of CAC improved risk stratification beyond existing, clinical risk scores. This was conclusively shown in the Heinz-Nixdorf RECALL included 4,487 subjects without known CAD. With the addition of CAC assessment to the Framingham-Risk-Score the area under the curve improved from 0.681 to 0.749 ($p<0.003$) and when CAC was added to the National Cholesterol Education Panel ATP III categories the area under the curve improved from 0.653 to 0.755 (18). CAC was a much stronger predictor of risk than carotid intima-media thickness, high-sensitivity C reactive protein and the ankle-brachial index (19). Further results from the MESA study showed that CAC improves risk assessment in individuals with family history (19). Consequently, CAC assessment has been incorporated into many clinical guidelines for risk stratification. Depending on the guideline used, CAC is considered an appropriate test to perform in asymptomatic adults at intermediate risk for heart disease. These patients are defined by having a 10%

to 20% 10-year risk or having a Systemic Coronary Risk evaluator (SCORE) (23) risk stratification value range of 5% - 10%, low-risk individuals with a family history of premature disease and all diabetic patients 40 years or older are also candidates for this test. (24-26) Budoff and colleagues (22) have recently shown that in the MESA cohort (N=6814) (<https://www.mesa-nhlbi.org/Calcium/input.aspx>) for each doubling of CAC there was a 14% increase in CVD risk. They concluded that CAC is highly associated with MACE and is this gated non contrast CT biomarker was found to be independent of standard risk factors (Supplementary Table S1).(22)

Evidence based guidelines for the use of CAC are based on publications using cardiac-gated CT. This is because CAC has a high density and is sensitive to motion artefacts leading to false CAC values (27). New technology of multi-detector computed tomography scanners with faster gantry rotation times and thinner detector row widths allow for thinner slices with a reduction in partial volume effects. These changes in hardware now allow for more exact and reliable measurement of CAC on non-gated NCCT scans (NG-NCCT). In a study by Wu et al (28) on 483 patients showed excellent correlation of Agatston CAC scores between a dedicated cardiac gated non-contrast CT for calcium scoring (16 slice multidetector, 3.0 mm slice thickness) and a low dose NG-NCCT (16 slice multidetector, 0.75mm slice thickness)performed for lung cancer screening (**Figure 1**). In their cohort of NG-NCCT patients the average heart was 61 beats per minute. They did not assess the importance of potential heart rate dependent motion artifact that may limit the accurate quantification of calcium score using non gated CT protocols.(28) They found an intraclass correlation coefficient of 0.95 for the agreement between the scores on low-dose NG-NCCT versus the respective routine cardiac-gated CT for CAC in this one observer study. In a study by Kim et al., where 128 patients underwent both non-gated low dose lung cancer screening and ECG-gated CAC scanning, an accuracy of 90% was observed for CAC>0 on the gated CAC scan and the absolute CAC scores correlated well ($r=0.89$) (29). In a meta-analysis of 661 subjects (3 separate studies) performed in 2013, Xie et al convincingly showed that, when the Agatston Score at non-gated low dose NCCT was compared with the gold standard of routine cardiac gated CT performed for CAC scoring, the pooled correlation coefficient was 0.94 (95%CI: 0.89-0.96). These data are confirmative of the newly available scatter plot from Wu et al(28) (**Figure 1**) showing a R^2 of 0.95 between Agatston scores as derived from NG-NCCT versus cardiac gated CT.

While the Agatston score as a continuous measurement has been established for formal CAC assessment, the development of visual scores for CAC categorization is essential in order to provide the chest radiologist with a simple technique that is less time consuming. Several studies have been performed showing that either a visual-qualitative assessment or a visual ordinal scale can be used for reliable and accurate risk assessment as compared to Agatston score (30-32). But more importantly, both Agatston score and/or a visual CAC assessment from NG-NCCT have prognostic value for cardiovascular events and overall mortality. In detail, a study performed by Mets et al in 3,648 lung cancer screening patients using an automatically derived Agatston score from NG-NCCT in a risk prediction model found overall good discrimination (AUC 0.71) with an event frequency of 12.2% vs 4.0% in the high vs. low risk groups, respectively.(33) In the ECLIPSE trial Williams et al found that CAC was increased in patients with chronic obstructive pulmonary disease and was associated with an increased risk of death.(34) In the National Lung Screening Trial assessing 1,442 patients (35), an Agatston scores of 1-100, 101-1000, and >1000 had HR of 1.27, 3.57, and 6.63 as derived from NG-NCCT and compared to an Agatston score of 0. Interestingly, in a case-control study authored by Hughes-Austin et al. in which both ECG-gated 3 mm and non-gated 6 mm CT scans were available, the predictive value of the Agatston score for mortality where similar.(36) Focusing on visual assessment, Shao et al showed in a single centre study that there is no significant difference in the discriminative power of visual CAC assessment vs. Agatston score (AUC: 0.80, 0.81).(37) Most evidence exist for a visual assessment using an ordinal CAC scoring system categorizing from 0-12 or 0-30 based upon visual estimation (**Table 1**). The study of Shemesh et al. including 8,782 smokers with 72 months mean follow up showed that this simple ordinal system was strongly predictive for cardiovascular death (32) and further confirmed by Blair et al. to be of similar predictive value as the Agatston score (31) (**Table 2**). Gonzales et al have recently shown that automated detection of Agatston scores can be derived from NG-NCCT exams.(38) Thus, in a common guideline, the Society of Cardiovascular Computed Tomography (SCCT) and the Society of Thoracic Radiology (STR) recommend “the incorporation of CAC into all non-gated non-contrast chest examination reports” since it “in the treatment of coronary artery disease“.(39)

It is very clear that coronary artery calcium can be reliably detected on NG-NCCT and that either ordinal scoring methods or quantification of the NG-NCCT Agatston score are highly correlated (within 10%) with those cardiac gated non-contrast CT exams that are performed only for CAC scoring. *An argument can be made that the*

CAC score value obtained using current state of the art multidetector NG- NCCT of the chest, performed for any reason, are a good proxy for a dedicated CAC scoring CT.

Aortic calcification

The thoracic aorta is another important vascular bed imaged on a standard chest CT. As compared to the coronary arteries, the assessment thoracic aorta calcification (TAC) less standardized but also less effected by cardiac motion. In a retrospective study by Jairam et al. found good predictive value for cardiovascular events when including visual assessment of TAC (HR: 0.37, $p < 0.001$) into a larger predicting model.(40) Similar results were observed in the Heinz Nixdorf RECALL study (41), where TAC together with other CT-derived parameters improved the prediction of events over the Framingham Risk Score and CAC (AUC: 0.749 to 0.764; $p = 0.01$). In contrast, Kim et al found in subjects from the MESA study without CAC ($n = 3,415$) that TAC was associated to cardiovascular events and all-cause mortality, but this association attenuated after adjustment for cardiovascular risk factors.(42) Similarly, in the Framingham Heart Study TAC provided no incremental value above risk factors for the prediction of events.(43) Thus, TAC is a prognostic marker, but its incremental value to traditional risk factors and other CT-findings, particular to CAC remain controversial.

Valvular Calcification

The most common valve affected by calcification is the aortic valve. The aortic valve calcification (AVC) can vary by its degree and/or by its location and can lead to aortic stenosis. The degree of stenosis is increasing with AVC extent, while calcification of the peripheral left-posterior and the central right-left commissural leaflets is particularly correlated with mean and peak gradient increases across the aortic valve.(44) The underlying pathophysiology is complex and integrates lipids, the renin-angiotensin system, inflammation, signalling pathways, and genetic predisposition.(45) Also, a strong linkage to visceral obesity has been described leading the neologism 'valvulo-metabolic' risk.(46) Further, AVC shares common risk factors with arteriosclerosis; hence, patients with AVC had more frequently coexisting presence of coronary plaque and had a greater extent of coronary plaque burden (6.4 vs 1.8 segments for patients with and without AVC, $P < 0.001$) as described in a study of 357 subjects undergoing cardiac

CT. (47) Interestingly, AVC was more strongly associated with calcified (OR: 5.2, $p=0.004$), then with mixed (OR: 3.2, $p=0.02$) or non-calcified plaque ($P=0.96$). Several studies have been performed regarding the prognostic value of AVC for cardiovascular events and all-cause mortality. Although AVC showed a prognostic value in univariate analysis, it attenuated in most studies after adjustment for traditional risk factors and after further adjustment for CAC and/or TAC.(43, 48-50)

Annular Calcification

The annulus of the mitral valve is most commonly calcified. Mitral annular calcification (MAC) is a chronic degenerative process in the fibrous base of the mitral valve and more commonly affects the posterior annulus than the anterior annulus. (51) Traditionally, MAC is assessed using echocardiography and several studies using this technology showed independent association of MAC with cardiac events.(52, 53) Given a good relationship in MAC between echocardiography and CT (54), MAC was also a good predictor for cardiovascular events if assessed by CT (55, 56). In the Northern Manhattan Study ($n=1,955$) (55), MAC prevalence was 27%, while severe MAC ($>4\text{mm}$ thickness) was observed in 13%. Presence of MAC was associated with myocardial infarction (HR: 1.75) and cardiac death (HR: 1.53) and these associations became stronger if using severe MAC as the predictor (HR: 1.89 and 1.81; respectively). In this cohort, but also in a cohort with atrial fibrillation, MAC was not significantly associated with cerebrovascular events. (55, 56)

Caseous calcification of the mitral valve is a rare form of MAC. The contents of the hollowed out cavity in the mitral valve annulus is composed of a mixture of calcium, fatty acids, and cholesterol that has a “toothpaste-like” texture. This commonly presents as an intracardiac mass at echocardiography. There is limited evidence regarding the prognostic value of caseous calcification of the mitral annulus. In a literature review of 1,502 articles, Dietl et al. identified a total of 130 patients with caseous calcification of the mitral annulus reported in 86 publications. The prevalence of cerebrovascular events was higher in patients with caseous calcification of the mitral annulus than with simple MAC (19% vs 12%, respectively; $p=0.02$).

Atrial and Ventricular size

There is a large body of evidence that MetS carries an increased risk of left ventricle (LV) hypertrophy, left atrial (LA) enlargement, systolic and/or diastolic dysfunction, arrhythmias and interstitial myocardial fibrosis. MetS is also associated with increased LV mass and LV diastolic dysfunction.(57, 58) CT can be useful for assessing cardiac chambers to determine their size, shape and thickness. Cardiac gated CT scans can usually be obtained during diastole for CAC scoring and coronary angiography, as this phase of the cardiac cycle has the least motion. While chamber assessment is relatively simple for gated, contrast-enhanced CT scans given existing software tools, NG-NCCT exams are more challenging and an area-based approach has been proposed. Schlett et al. showed that an area-based measurement for LV on axial, non-contrast enhanced CT images correlates well with LV volume, mass and size ($r=0.68$; $r=0.73$; $r=0.82$). (59) Similar correlations were observed for the left atrium. (60) In the MESA cohort, such area-based LV measurement of non-contrast CT scans is a predictor of incident heart failure events (HR 1.15; 95%CI 1.11-1.20) beyond traditional risk factors and CAC score; but also for CHD events (HR 1.07; 95%CI 1.03-1.10). As RV and LV contraction is usually synchronous, the RV/LV diameter and volume ratios have been used in NG-NCCT studies to assess RV dilation and dysfunction in response to increased RV afterload. (Henzler et al 2012, Mansencal et al. 2005) A limited number of reports indicate that RV hypertrophy may parallel alterations in LV structure and function in the setting of systemic hypertension, obesity and diabetes. (Chahal et al 2012) All the components of MetS (increased blood pressure, abdominal obesity, increased fasting glucose level and dyslipidemia) may induce right ventricular remodelling by several hemodynamic and non-hemodynamic mechanisms. (Tadic et al. 2013) Increasing evidence suggests that in pulmonary hypertension (PH) RV dysfunction is associated with various components of MetS, such as insulin resistance, hyperglycemia, and dyslipidemia. (Talati et al. 2015)

Regarding LA assessment, an enlarged size was associated with a 3- to 5-fold increase risk for ACS and provided incremental value for predicting ACS when added to the CT finding of indeterminate coronary artery stenosis in a population with acute chest pain presenting to the ED. (61) In the Heinz-Nixdorf Recall Study (62), LA size had prognostic value (HR 1.48), which remained significant after adjustment for traditional risk factors (HR 95%CI: 1.09-1.43) and after adjustment for traditional risk factors plus CAC (HR 95%CI: 1.07-1.40) (**Table 2**). Prognostic value of LA size was similar for different endpoints (coronary event: HR: 1.21; stroke: 1.31; CV death: 1.33). LA size also remained associated with cardiovascular events independent of other CT non-coronary

findings.(41) Recently Jivraj et al have shown in 165 patients with right heart catheterization proven pulmonary hypertension (PAP > 45 mm Hg) and capillary wedge pressures (43 patients - PCWP > 15 mm Hg, 122 patients PCWP < 15 mm Hg) that left atrial maximal cross-sectional area (LA-MACSA) measured from NG-NCCT (LA-MACSA > 2400mm², P<0.001) had a 44% sensitivity and 93% specificity for pulmonary hypertension from left heart disease.(63) On NG-NCCT studies the images may not reveal the true ventricular morphology because the phase of the cardiac cycle is unknown. However, a few studies have reported good sensitivity and specificity (both >68%) of standard axial, non-gated chest CT for cardiomyopathies. (64)

Left ventricle

The left ventricle size (volume and in-plane area) can be estimated from NCCT chest exams. Bhatt and colleagues (65) have created an automated process for generating the expected ventricular sizes from NG-NCCT chest exams by comparing these studies to ultrasound and cardiovascular MRI exams that show the ventricular volumes and wall thickness (Supplemental Figure 1). The assessment of ventricular volume and wall thickness is easier if the patient is anemic, as the ventricular chambers are seen to be of lower Hounsfield unit density than the walls. The presence of prior left ventricular myocardial infarction is also easily determined by the presence of a low density scar (**Figure 3**). These are typically seen in the subendocardial regions of the wall and may be transmural.

Recently Kockelkoren et al published their data from routine NG-NCCT exams on patients that were studied for non-cardiovascular disease (**Tables 3 and 4**). This was derived from a rather homogeneous population of Caucasians in the United Kingdom. This group of researchers created a simple to use ordinal grading scale for the determination of future major adverse cardiac events (MACE) (**Table 3**) and have a computational model for the likelihood of a major cardiac event within 5 years that is based on a best fit multivariable regression model (**Supplementary Tables S2, S3**). The parameters include: age, male gender, indication for exam, left anterior descending coronary artery calcium (LAD Ca++) value, mitral valve leaflet calcification (MV Ca++) value, descending aorta calcium value (DSC Ca++), and the maximum transverse diameter (cm) of the heart.

Epicardial Fat

In their study of 3,630 subjects from the Heinz-Nixdorf Recall Study, Mahabadi et al(41) found that the epicardial fat volume (HR: 1.15, 95% C.I 1.01-1.30, p value 0.03), was an imaging biomarker predictive of myocardial infarction, stroke and cardiovascular death (**Table 5**). In their systematic review, Bertaso et al found that the heterogeneity of the studies limits the conclusions that can be drawn from using this metric. They found that this visceral fat deposit is highly correlated with obesity, diabetes mellitus, age and hypertension. Manno et al showed that epicardial fat thickness at ultrasound was correlated with higher LDL cholesterol.(66) In their study from 2018, Hedgire et al show that perivascular fat stranding, seen on coronary CT angiography is associated with high risk clinical features and they suggest that fat stranding is a potential imaging biomarker of high-risk and/or ruptured atherosclerotic plaques.(67) Hartiala et al found no evidence that increased epicardial fat volume was independently associated with pre-clinical atherosclerosis.(68) Instead, they found that epicardial fat volume was primarily associated with BMI and waist circumference.(68) Furthermore, there is increasing evidence that fat quality rather fat volume may play a role in the association to CVD. (69)

Pulmonary artery diameter predicts pulmonary hypertension

Sleep disordered breathing (sleep apnea) is an important cause of pulmonary hypertension.(70) Obstructive Sleep Apnea (OSA) is caused by the increased collapsibility of the upper airway from loss of muscle tone and a decrease in the effective orifice from fat deposition in the tongue and surrounding pharynx during sleep.(71) This results in decreased or absent airflow and hypoxia. These episodes are usually terminated by a brief arousal from sleep and resulting in sleep deprivation for subjects with MetS.(72) Over many years, these apneic episodes lead to sleep fragmentation and altered cognitive function. (73) These episodes of hypoxia are associated with pulmonary artery vasoconstriction and can lead to permanent changes in PA size (**Figure 5**).(74) Corson et al studied 175 subjects with right heart catheterization (RHC) proven pulmonary hypertension (PH), 16 normal patients with proven normal mean pulmonary artery pressures (mPAP) and 114 subjects without known mPAP and found a sensitivity of the criterion “mean pulmonary artery diameter at the level of the bifurcation >29mm” was 0.89 (95% C.I. 0.84-0.93) and a specificity of 0.83 (95%CI: 0.76-0.90).(75) Truong et al studied 706 “healthy cohort” subjects in the Framingham Heart Study using cardiac gated NCCT and found a 90th percentile cut-off value of 28.9 mm in men and 26.9 mm in women.(76) Pulmonary artery diameter is an important clue that may indicate pulmonary

hypertension from any cause (77); in the setting of obesity or MetS an enlarged PA can be used to alert the imager and clinician to the possibility for OSA. Instituting treatment with Continuous Positive Airway Pressure (CPAP) can significantly improve the length and quality of life for these individuals.

Radiation dose and safety using NG-NCCT for the diagnosis of MetS

We are not proposing to use NCCT for the diagnosis of MetS or obesity. From studies performed for other indications, the imaging physician can also make inferences about the metabolic milieu of that subject based on the multiple imaging findings discussed in this review. For the most part low dose chest CT protocols are very low contributors to the medical radiation any patient receives over the course of their lifetime.(78) Each scan delivers between 0.5 and 5 mSv depending on the patient size, use of dose lowering reconstruction methods and automatic exposure control (limit mAs).(79)

Conclusion

The beauty of non-gated, non-contrast computed of the chest is that quantitative assessment of Hounsfield unit density, contour and volume of many organs can be assessed longitudinally and correlated to patient outcomes. This differs substantially from contrast enhanced CT data, because there is no iodinated contrast material confounding the density measurements. There are easy to access imaging biomarkers associated with obesity, atherosclerotic disease and MetS that are routinely seen on these exams. The most important one found on NG-NCCT is coronary artery calcification. Various models combining clinical and imaging data have been shown to have prognostic significance for Major Adverse Cardiac Events. Thus, these exams are a virtual treasure trove of quantitative imaging biomarker information available for retrospective analysis to create survival models (training sets) that can be applied prospectively to test sets and validated with external data sets. These big data can be added to radiomic feature analysis, convolutional neural networks and/or added to deep neural networks without any user defined features to create better survival models that can be used to help design personalized medical interventions aimed at prolonging quality life expectancy.

References

1. Mortality GBD, Causes of Death C. Global, regional, and national life expectancy, all-cause mortality, and cause-specific mortality for 249 causes of death, 1980-2015: a systematic analysis for the Global Burden of Disease Study 2015. *Lancet*. 2016;388(10053):1459-544.
2. Alberti KG, Eckel RH, Grundy SM, et al. Harmonizing the metabolic syndrome: a joint interim statement of the International Diabetes Federation Task Force on Epidemiology and Prevention; National Heart, Lung, and Blood Institute; American Heart Association; World Heart Federation; International Atherosclerosis Society; and International Association for the Study of Obesity. *Circulation*. 2009;120(16):1640-5.
3. Bizino MB, Sala ML, de Heer P, et al. MR of multi-organ involvement in the metabolic syndrome. *Magn Reson Imaging Clin N Am*. 2015;23(1):41-58.
4. de Clercq NC, Frissen MN, Groen AK, Nieuwdorp M. Gut Microbiota and the Gut-Brain Axis: New Insights in the Pathophysiology of Metabolic Syndrome. *Psychosom Med*. 2017;79(8):874-9.
5. Peters MC, Fahy JV. Metabolic consequences of obesity as an "outside in" mechanism of disease severity in asthma. *Eur Respir J*. 2016;48(2):291-3.
6. Peters MC, McGrath KW, Hawkins GA, et al. Plasma interleukin-6 concentrations, metabolic dysfunction, and asthma severity: a cross-sectional analysis of two cohorts. *Lancet Respir Med*. 2016;4(7):574-84.
7. Ng M, Fleming T, Robinson M, et al. Global, regional, and national prevalence of overweight and obesity in children and adults during 1980-2013: a systematic analysis for the Global Burden of Disease Study 2013. *Lancet*. 2014;384(9945):766-81.
8. Schwimmer JB. Definitive diagnosis and assessment of risk for nonalcoholic fatty liver disease in children and adolescents. *Semin Liver Dis*. 2007;27(3):312-8.
9. Imhof A, Kratzer W, Boehm B, et al. Prevalence of non-alcoholic fatty liver and characteristics in overweight adolescents in the general population. *Eur J Epidemiol*. 2007;22(12):889-97.
10. Eckel RH, Grundy SM, Zimmet PZ. The metabolic syndrome. *Lancet*. 2005;365(9468):1415-28.
11. Madaj P, Budoff MJ. Risk stratification of non-contrast CT beyond the coronary calcium scan. *J Cardiovasc Comput Tomogr*. 2012;6(5):301-7.
12. Bastos M, Lee EY, Strauss KJ, Zurakowski D, Tracy DA, Boisselle PM. Motion artifact on high-resolution CT images of pediatric patients: comparison of volumetric and axial CT methods. *AJR American journal of roentgenology*. 2009;193(5):1414-8.
13. Yanagawa M, Tomiyama N, Sumikawa H, et al. Thin-section CT of lung without ECG gating: 64-detector row CT can markedly reduce cardiac motion artifact which can simulate lung lesions. *Eur J Radiol*. 2009;69(1):102-7.
14. Ko SF, Hsieh MJ, Chen MC, et al. Effects of heart rate on motion artifacts of the aorta on non-ECG-assisted 0.5-sec thoracic MDCT. *AJR American journal of roentgenology*. 2005;184(4):1225-30.
15. Fukuda A, Lin PJ, Matsubara K, Miyati T. Measurement of gantry rotation time in modern ct. *J Appl Clin Med Phys*. 2014;15(1):4517.
16. Bertheau RC, Bamberg F, Lochner E, et al. Whole-Body MR Imaging Including Angiography: Predicting Recurrent Events in Diabetics. *European radiology*. 2016;26(5):1420-30.
17. Sverzellati N, Arcadi T, Salvolini L, et al. Under-reporting of cardiovascular findings on chest CT. *La Radiologia medica*. 2016;121(3):190-9.

18. Erbel R, Mohlenkamp S, Moebus S, et al. Coronary risk stratification, discrimination, and reclassification improvement based on quantification of subclinical coronary atherosclerosis: the Heinz Nixdorf Recall study. *Journal of the American College of Cardiology*. 2010;56(17):1397-406.
19. Yeboah J, McClelland RL, Polonsky TS, et al. Comparison of novel risk markers for improvement in cardiovascular risk assessment in intermediate-risk individuals. *JAMA*. 2012;308(8):788-95.
20. Detrano R, Guerci AD, Carr JJ, et al. Coronary calcium as a predictor of coronary events in four racial or ethnic groups. *The New England journal of medicine*. 2008;358(13):1336-45.
21. Baber U, Mehran R, Sartori S, et al. Prevalence, impact, and predictive value of detecting subclinical coronary and carotid atherosclerosis in asymptomatic adults: the BioImage study. *Journal of the American College of Cardiology*. 2015;65(11):1065-74.
22. Budoff MJ, Young R, Burke G, et al. Ten-year association of coronary artery calcium with atherosclerotic cardiovascular disease (ASCVD) events: the multi-ethnic study of atherosclerosis (MESA). *Eur Heart J*. 2018;39(25):2401-8.
23. Perk J, De Backer G, Gohlke H, et al. European Guidelines on cardiovascular disease prevention in clinical practice (version 2012): The Fifth Joint Task Force of the European Society of Cardiology and Other Societies on Cardiovascular Disease Prevention in Clinical Practice (constituted by representatives of nine societies and by invited experts). *Atherosclerosis*. 2012;223(1):1-68.
24. Piepoli MF, Hoes AW, Agewall S, et al. 2016 European Guidelines on cardiovascular disease prevention in clinical practice: The Sixth Joint Task Force of the European Society of Cardiology and Other Societies on Cardiovascular Disease Prevention in Clinical Practice (constituted by representatives of 10 societies and by invited experts) Developed with the special contribution of the European Association for Cardiovascular Prevention & Rehabilitation (EACPR). *European heart journal*. 2016;37(29):2315-81.
25. Greenland P, Alpert JS, Beller GA, et al. 2010 ACCF/AHA guideline for assessment of cardiovascular risk in asymptomatic adults: executive summary: a report of the American College of Cardiology Foundation/American Heart Association Task Force on Practice Guidelines. *Circulation*. 2010;122(25):2748-64.
26. Taylor AJ, Cerqueira M, Hodgson JM, et al. ACCF/SCCT/ACR/AHA/ASE/ASNC/NASCI/SCAI/SCMR 2010 Appropriate Use Criteria for Cardiac Computed Tomography. A Report of the American College of Cardiology Foundation Appropriate Use Criteria Task Force, the Society of Cardiovascular Computed Tomography, the American College of Radiology, the American Heart Association, the American Society of Echocardiography, the American Society of Nuclear Cardiology, the North American Society for Cardiovascular Imaging, the Society for Cardiovascular Angiography and Interventions, and the Society for Cardiovascular Magnetic Resonance. *J Cardiovasc Comput Tomogr*. 2010;4(6):407 e1-33.
27. Brown SJ, Hayball MP, Coulden RA. Impact of motion artefact on the measurement of coronary calcium score. *Br J Radiol*. 2000;73(873):956-62.
28. Wu MT, Yang P, Huang YL, et al. Coronary arterial calcification on low-dose ungated MDCT for lung cancer screening: concordance study with dedicated cardiac CT. *AJR American journal of roentgenology*. 2008;190(4):923-8.
29. Kim SM, Chung MJ, Lee KS, Choe YH, Yi CA, Choe BK. Coronary calcium screening using low-dose lung cancer screening: effectiveness of MDCT with retrospective reconstruction. *AJR Am J Roentgenol*. 2008;190(4):917-22.
30. Htwe Y, Cham MD, Henschke CI, et al. Coronary artery calcification on low-dose computed tomography: comparison of Agatston and Ordinal Scores. *Clin Imaging*. 2015;39(5):799-802.
31. Blair KJ, Allison MA, Morgan C, et al. Comparison of ordinal versus Agatston coronary calcification scoring for cardiovascular disease mortality in community-living individuals. *Int J Cardiovasc Imaging*. 2014;30(4):813-8.

32. Shemesh J, Henschke CI, Shaham D, et al. Ordinal scoring of coronary artery calcifications on low-dose CT scans of the chest is predictive of death from cardiovascular disease. *Radiology*. 2010;257(2):541-8.
33. Mets OM, Vliegenthart R, Gondrie MJ, et al. Lung cancer screening CT-based prediction of cardiovascular events. *JACC Cardiovasc Imaging*. 2013;6(8):899-907.
34. Williams MC, Murchison JT, Edwards LD, et al. Coronary artery calcification is increased in patients with COPD and associated with increased morbidity and mortality. *Thorax*. 2014;69(8):718-23.
35. Chiles C, Duan F, Gladish GW, et al. Association of Coronary Artery Calcification and Mortality in the National Lung Screening Trial: A Comparison of Three Scoring Methods. *Radiology*. 2015;276(1):82-90.
36. Hughes-Austin JM, Dominguez A, 3rd, Allison MA, et al. Relationship of Coronary Calcium on Standard Chest CT Scans With Mortality. *JACC Cardiovasc Imaging*. 2016;9(2):152-9.
37. Shao L, Yan AT, Lebovic G, Wong HH, Kirpalani A, Deva DP. Prognostic value of visually detected coronary artery calcification on unenhanced non-gated thoracic computed tomography for prediction of non-fatal myocardial infarction and all-cause mortality. *J Cardiovasc Comput Tomogr*. 2017;11(3):196-202.
38. Gonzalez G, Washko GR, Estepar RS. Automated Agatston Score Computation in a Large Dataset of Non Ecg-Gated Chest Computed Tomography. *Proc IEEE Int Symp Biomed Imaging*. 2016;2016:53-7.
39. Hecht HS, Cronin P, Blaha MJ, et al. 2016 SCCT/STR guidelines for coronary artery calcium scoring of noncontrast noncardiac chest CT scans: A report of the Society of Cardiovascular Computed Tomography and Society of Thoracic Radiology. *Journal of thoracic imaging*. 2017;32(5):W54-W66.
40. Jairam PM, Gondrie MJ, Grobbee DE, et al. Incidental imaging findings from routine chest CT used to identify subjects at high risk of future cardiovascular events. *Radiology*. 2014;272(3):700-8.
41. Mahabadi AA, Lehmann N, Mohlenkamp S, et al. Noncoronary Measures Enhance the Predictive Value of Cardiac CT Above Traditional Risk Factors and CAC Score in the General Population. *JACC Cardiovascular imaging*. 2016;9(10):1177-85.
42. Kim J, Budoff MJ, Nasir K, et al. Thoracic aortic calcium, cardiovascular disease events, and all-cause mortality in asymptomatic individuals with zero coronary calcium: The Multi-Ethnic Study of Atherosclerosis (MESA). *Atherosclerosis*. 2017;257:1-8.
43. Hoffmann U, Massaro JM, D'Agostino RB, Sr., Kathiresan S, Fox CS, O'Donnell CJ. Cardiovascular Event Prediction and Risk Reclassification by Coronary, Aortic, and Valvular Calcification in the Framingham Heart Study. *J Am Heart Assoc*. 2016;5(2).
44. Liu F, Coursey CA, Grahame-Clarke C, et al. Aortic valve calcification as an incidental finding at CT of the elderly: severity and location as predictors of aortic stenosis. *AJR Am J Roentgenol*. 2006;186(2):342-9.
45. O'Brien KD. Pathogenesis of calcific aortic valve disease: a disease process comes of age (and a good deal more). *Arterioscler Thromb Vasc Biol*. 2006;26(8):1721-8.
46. Mathieu P, Despres JP, Pibarot P. The 'valvulo-metabolic' risk in calcific aortic valve disease. *Can J Cardiol*. 2007;23 Suppl B:32B-9B.
47. Mahabadi AA, Bamberg F, Toepker M, et al. Association of aortic valve calcification to the presence, extent, and composition of coronary artery plaque burden: from the Rule Out Myocardial Infarction using Computer Assisted Tomography (ROMICAT) trial. *Am Heart J*. 2009;158(4):562-8.
48. Revilla-Orodea A, Toro-Gil JA, Sevilla T, et al. Coronary artery and aortic valve calcification evaluated with cardiac computed tomography in patients with chest pain: Prognostic value in clinical practice. *Int J Cardiol*. 2016;219:247-50.
49. Willemink MJ, Takx RA, Isgum I, et al. Prognostic value of heart valve calcifications for cardiovascular events in a lung cancer screening population. *Int J Cardiovasc Imaging*. 2015;31(6):1243-9.

50. Gondrie MJ, van der Graaf Y, Jacobs PC, Oen AL, Mali WP, Group PS. The association of incidentally detected heart valve calcification with future cardiovascular events. *European radiology*. 2011;21(5):963-73.
51. Abramowitz Y, Jilaihawi H, Chakravarty T, Mack MJ, Makkar RR. Mitral Annulus Calcification. *Journal of the American College of Cardiology*. 2015;66(17):1934-41.
52. Fox CS, Vasan RS, Parise H, et al. Mitral annular calcification predicts cardiovascular morbidity and mortality: the Framingham Heart Study. *Circulation*. 2003;107(11):1492-6.
53. Holtz JE, Upadhyaya DS, Cohen BE, Na B, Schiller NB, Whooley MA. Mitral annular calcium, inducible myocardial ischemia, and cardiovascular events in outpatients with coronary heart disease (from the Heart and Soul Study). *Am J Cardiol*. 2012;109(8):1092-6.
54. Mahnken AH, Muhlenbruch G, Das M, et al. MDCT detection of mitral valve calcification: prevalence and clinical relevance compared with echocardiography. *AJR Am J Roentgenol*. 2007;188(5):1264-9.
55. Kohsaka S, Jin Z, Rundek T, et al. Impact of mitral annular calcification on cardiovascular events in a multiethnic community: the Northern Manhattan Study. *JACC Cardiovasc Imaging*. 2008;1(5):617-23.
56. Potpara TS, Vasiljevic ZM, Vujisic-Tesic BD, et al. Mitral annular calcification predicts cardiovascular morbidity and mortality in middle-aged patients with atrial fibrillation: the Belgrade Atrial Fibrillation Study. *Chest*. 2011;140(4):902-10.
57. Aijaz B, Ammar KA, Lopez-Jimenez F, Redfield MM, Jacobsen SJ, Rodeheffer RJ. Abnormal cardiac structure and function in the metabolic syndrome: a population-based study. *Mayo Clin Proc*. 2008;83(12):1350-7.
58. Ladeiras-Lopes R, Moreira HT, Bettencourt N, et al. Metabolic Syndrome Is Associated With Impaired Diastolic Function Independently of MRI-Derived Myocardial Extracellular Volume: The MESA Study. *Diabetes*. 2018;67(5):1007-12.
59. Schlett CL, Kwiat DC, Mahabadi AA, et al. Simple area-based measurement for multidetector computed tomography to predict left ventricular size. *European radiology*. 2010;20(7):1590-6.
60. Mahabadi AA, Truong QA, Schlett CL, et al. Axial area and anteroposterior diameter as estimates of left atrial size using computed tomography of the chest: comparison with 3-dimensional volume. *J Cardiovasc Comput Tomogr*. 2010;4(1):49-54.
61. Truong QA, Bamberg F, Mahabadi AA, et al. Left atrial volume and index by multi-detector computed tomography: comprehensive analysis from predictors of enlargement to predictive value for acute coronary syndrome (ROMICAT study). *Int J Cardiol*. 2011;146(2):171-6.
62. Mahabadi AA, Geisel MH, Lehmann N, et al. Association of computed tomography-derived left atrial size with major cardiovascular events in the general population: the Heinz Nixdorf Recall Study. *Int J Cardiol*. 2014;174(2):318-23.
63. Jivraj K, Bedayat A, Sung YK, et al. Left Atrium Maximal Axial Cross-Sectional Area is a Specific Computed Tomographic Imaging Biomarker of World Health Organization Group 2 Pulmonary Hypertension. *Journal of thoracic imaging*. 2017;32(2):121-6.
64. Murphy DJ, Lavelle LP, Gibney B, O'Donohoe RL, Remy-Jardin M, Dodd JD. Diagnostic accuracy of standard axial 64-slice chest CT compared to cardiac MRI for the detection of cardiomyopathies. *Br J Radiol*. 2016;89(1059):20150810.
65. Bhatt SP, Vegas-Sanchez-Ferrero G, Rahaghi FN, et al. Cardiac Morphometry on Computed Tomography and Exacerbation Reduction with beta-Blocker Therapy in Chronic Obstructive Pulmonary Disease. *Am J Respir Crit Care Med*. 2017;196(11):1484-8.
66. Manno C, Campobasso N, Nardecchia A, et al. Relationship of para- and perirenal fat and epicardial fat with metabolic parameters in overweight and obese subjects. *Eat Weight Disord*. 2018.

67. Hedgire S, Baliyan V, Zucker EJ, et al. Perivascular Epicardial Fat Stranding at Coronary CT Angiography: A Marker of Acute Plaque Rupture and Spontaneous Coronary Artery Dissection. *Radiology*. 2018;287(3):808-15.
68. Hartiala O, Magnussen CG, Bucci M, et al. Coronary heart disease risk factors, coronary artery calcification and epicardial fat volume in the Young Finns Study. *Eur Heart J Cardiovasc Imaging*. 2015;16(11):1256-63.
69. Antonopoulos AS, Sanna F, Sabharwal N, et al. Detecting human coronary inflammation by imaging perivascular fat. *Sci Transl Med*. 2017;9(398).
70. Nakamoto T. Sleep-Disordered Breathing-a Real Therapeutic Target for Hypertension, Pulmonary Hypertension, Ischemic Heart Disease, and Chronic Heart Failure? *J Nippon Med Sch*. 2018;85(2):70-7.
71. Kim AM, Keenan BT, Jackson N, et al. Tongue fat and its relationship to obstructive sleep apnea. *Sleep*. 2014;37(10):1639-48.
72. Mazzuca E, Battaglia S, Marrone O, et al. Gender-specific anthropometric markers of adiposity, metabolic syndrome and visceral adiposity index (VAI) in patients with obstructive sleep apnea. *J Sleep Res*. 2014;23(1):13-21.
73. Leng Y, McEvoy CT, Allen IE, Yaffe K. Association of Sleep-Disordered Breathing With Cognitive Function and Risk of Cognitive Impairment: A Systematic Review and Meta-analysis. *JAMA Neurol*. 2017;74(10):1237-45.
74. Dobrowolski P, Florczak E, Klisiewicz A, et al. Pulmonary artery dilation indicates severe obstructive sleep apnea in patients with resistant hypertension: the Resist-POL Study. *Pol Arch Med Wewn*. 2016;126(4):222-9.
75. Corson N, Armato SG, Labby ZE, Straus C, Starkey A, Gomberg-Maitland M. CT-based pulmonary artery measurements for the assessment of pulmonary hypertension. *Academic radiology*. 2014;21(4):523-30.
76. Truong QA, Massaro JM, Rogers IS, et al. Reference values for normal pulmonary artery dimensions by noncontrast cardiac computed tomography: the Framingham Heart Study. *Circ Cardiovasc Imaging*. 2012;5(1):147-54.
77. Renapurkar RD, Shrikanthan S, Heresi GA, Lau CT, Gopalan D. Imaging in Chronic Thromboembolic Pulmonary Hypertension. *Journal of thoracic imaging*. 2017;32(2):71-88.
78. Tabari A, Lo Gullo R, Murugan V, Otrakji A, Digumarthy S, Kalra M. Recent Advances in Computed Tomographic Technology: Cardiopulmonary Imaging Applications. *Journal of thoracic imaging*. 2017;32(2):89-100.
79. Padole A, Singh S, Ackman JB, et al. Submillisievert chest CT with filtered back projection and iterative reconstruction techniques. *AJR American journal of roentgenology*. 2014;203(4):772-81.
80. Shemesh J. Coronary artery calcification in clinical practice: what we have learned and why should it routinely be reported on chest CT? *Ann Transl Med*. 2016;4(8):159.
81. Kockelkoren R, Jairam PM, Murchison JT, et al. Validation of an imaging based cardiovascular risk score in a Scottish population. *Eur J Radiol*. 2018;98:143-9.

Legends

Legend Figure 1: Data from Wu et al (28) in a study comparing Agatston Calcium Scores on non-cardiac gated, non-contrast low dose CT (LDCT) performed for lung cancer screening to standard cardiac gated, non-contrast computed tomography (NCCT) in 513 consecutive cases. This shows excellent correlation between these two ways to quantify Agatston coronary artery calcification scores ($R^2=0.95$). They found a systematic under quantification of CAC using LDCT (y intercept = -12.1). Thus, any coronary artery calcification found at LDCT is worthy of quantification. This can be performed either by ordinal scoring or using post processing to obtain the non-cardiac gated LDCT Agatston score. (Scatter plot of the raw data made expressly for this article by Ming-Ting Wu, M.D.)

Legend Figure 2: Non gated, non-contrast computed tomography of the chest with globular calcification of an atherosclerotic plaque at the origin of the left anterior descending coronary artery (arrow head).

Legend Figure 3: Non-gated, non-contrast computed tomography of the chest coned down to the heart (A) axial and (B) short axis reconstruction showing a fibrofatty subendocardial scar (arrows) in the left ventricular septum, inferior and inferolateral walls from an old myocardial infarction in the right coronary artery vascular territory. Note the presence of hepatic steatosis as well (A) with a liver density of 35 Hounsfield units (ROI -Region of interest).

Legend Figure 4: 45 year old Caucasian male with(A) borderline evidence for low iodine organification in the thyroid with a thyroid density of 64 (Normal range 80-120 HU) (B) non gated Agatston score of 2 is at least in the 79th percentile for age and sex. There was hepatic steatosis as well (C) with a liver density of 42.9 HU. The

paraspinous muscle density was low measuring 33.8 HU at the T12 level (Normal range 5-60HU, from unpublished data (Tsuchiya et al, submitted)). This constellation of findings is the imaging equivalent of the clinically defined Metabolic Syndrome and suggests both glucose intolerance and an increase in overall inflammatory cytokines due to the low paraspinous muscle density.

Legend Figure 5: Pulmonary trunk measured at the largest part of the right main pulmonary artery is 4.0 cm (white line). This is abnormal and is suggestive of the possibility of pulmonary hypertension/pulmonary arterial hypertension. In an obese individual a common cause is sleep disordered breathing (sleep apnea) which can be treated with a night time Continuous Positive Airway Pressure (CPAP) mask.

Legend Supplemental Figure 1: Automatic segmentation of the left and right ventricular cavities from non contrast non cardiac gated chest CT exams using the method of Bhatt et al (65), (A) axial chest CT with the estimated left ventricle cavity in light red and the estimated left ventricular wall in dark red, with the estimated right ventricle in blue, (B) sagittal non contrast CT showing the estimated left ventricle in red and the estimated right ventricle in blue. (C) coronal chest CT showing the estimated left ventricle in red and the estimated right ventricle in blue, (D) Entire volume of left ventricle in red and right ventricle in blue.

Legend Table 1: Importance of coronary artery calcification found on non-cardiac gated chest computed tomography in patients that smoke cigarettes (table modified from Shemesh et al) (80) Practical comments for chest radiologists showing that the larger ordinal coronary artery calcium score is associated with an increased risk of Major Adverse Cardiac Events. (This table is modified from Shemesh et al (80)) Abbreviations: CAC- coronary artery calcium score; Visual Score (Likert Scale range from 0-12); CAD- coronary artery disease, PVD- peripheral vascular disease;

Legend Table 2: Imaging findings on non-contrast, non-cardiac gated Chest Computed tomography exams that are reflective of individual biology and the metabolic syndrome. (Abbreviations: n- number affected. N=total in study)

Legend Table 3: Imaging based cardiovascular risk biomarkers derived from a Caucasian population in Scotland (N=2124) (81). This type of analytic approach to documenting vascular calcifications was first used by Jairam et al in 2014 (40).

Legend Table 4: Hazard Ratios for the most significant model parameters for determining cardiovascular risk from contrast enhanced, non-gated chest CT exams from the PROVIDI study (N=10,410) (40).

Legend Table 5: Multivariable analysis of clinical and imaging based cardiovascular risk biomarkers derived from 3,630 subjects enrolled in the prospectively acquired Hienz-Nixdorff Recall Study. (41) and their adjusted Hazard Ratios for the interval development of major adverse cardiac events (MACE). (Abbreviations: FR- Framingham Risk Score, CAC- Coronary artery Agatston Score,)

Legend Table S1: Multi-Ethnic Study of Atherosclerosis (MESA) results from Budoff et al(22) modified from Table 2 in the original publication, showing the ten year event rate of major adverse cardiac events based simply off of the gated CT chest coronary artery Agatston calcium scores. These event rates are not adjusted for any clinical risk factors. These data show the effects of CAC transcend age related changes; in that more CAC is worse than simply being old. The Chinese and Caucasian were less affected by CAC than African-Americans and Hispanics.

Legend Tables S2 and S3: Kockelkoren (81) Scottish heart study risk 10 year estimated risk model (Table S2) and the equation used to derive the 5 year risk score (Table S3)

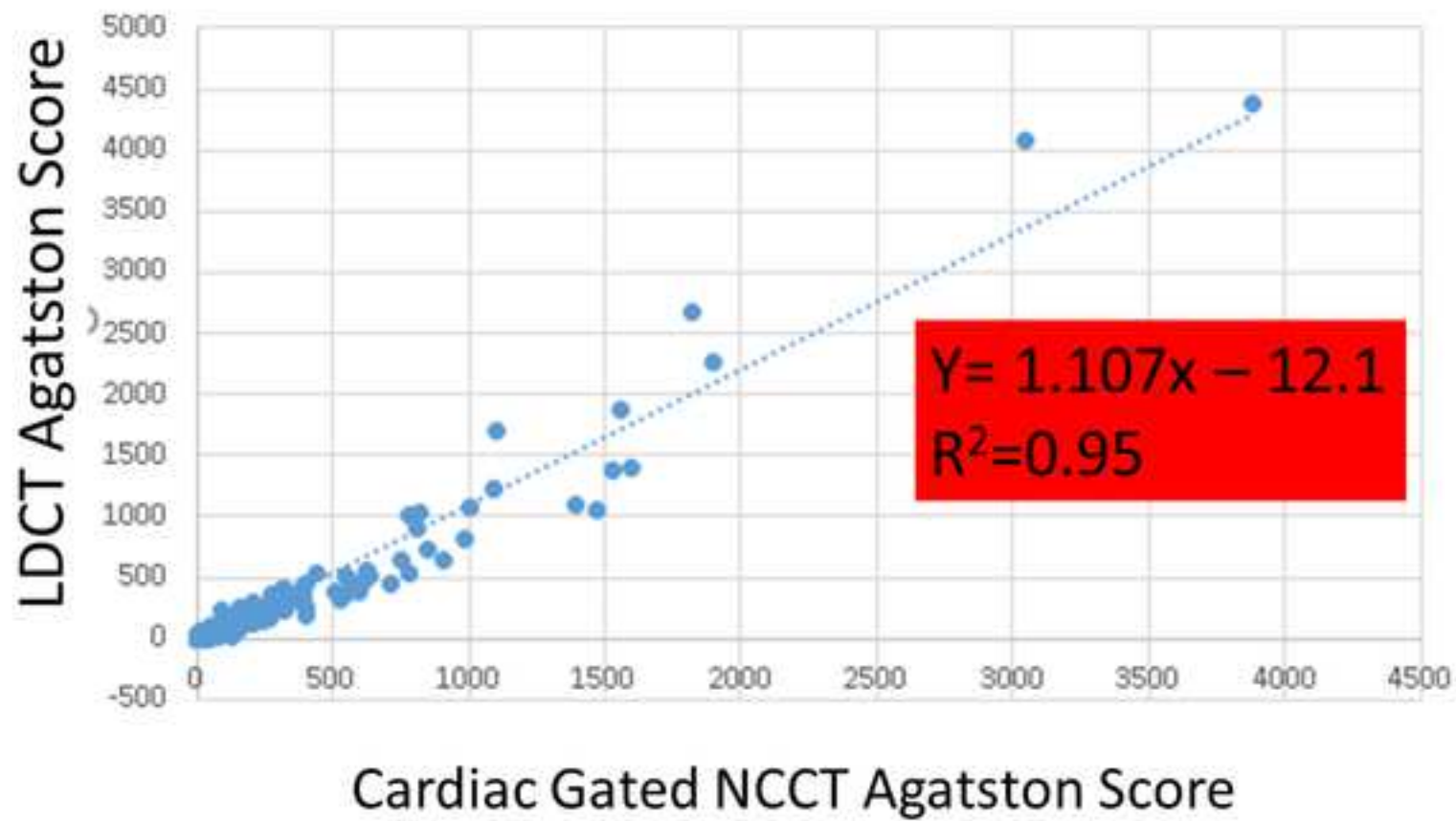


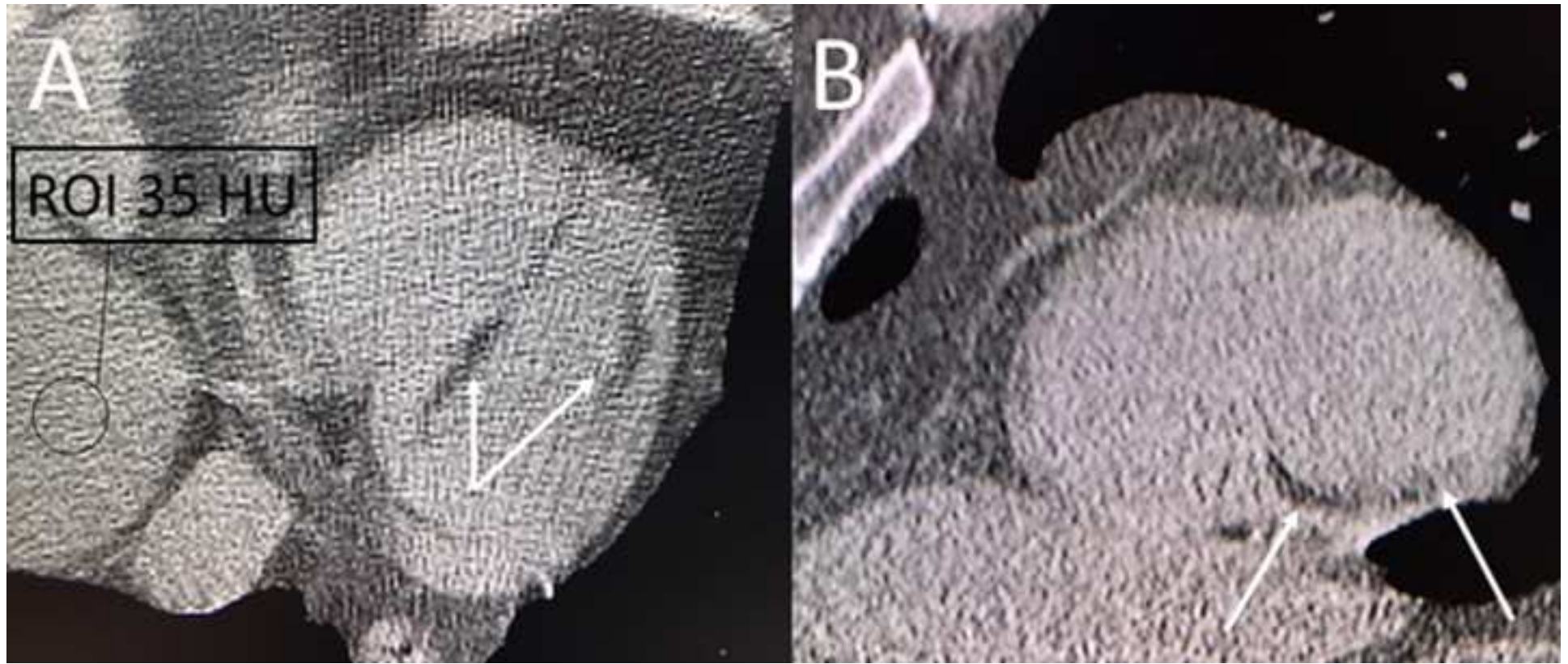
Figure 2

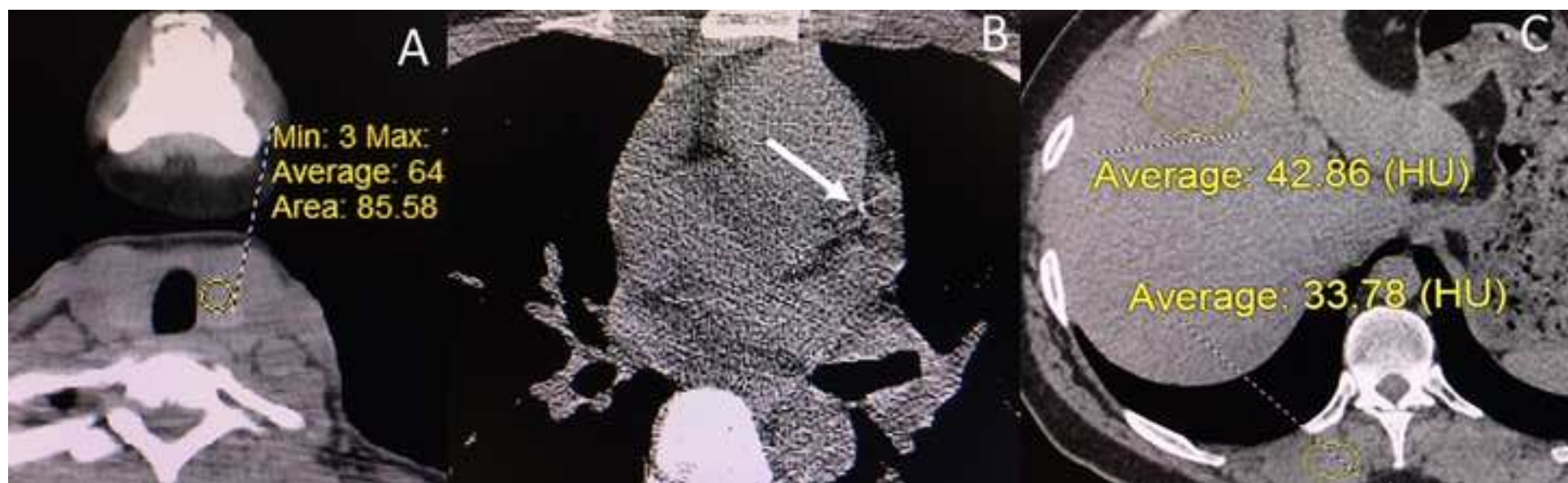
[Click here to access/download;Figure;Mets figure 2 LAD Ca++ 600 dpi.tif](#)

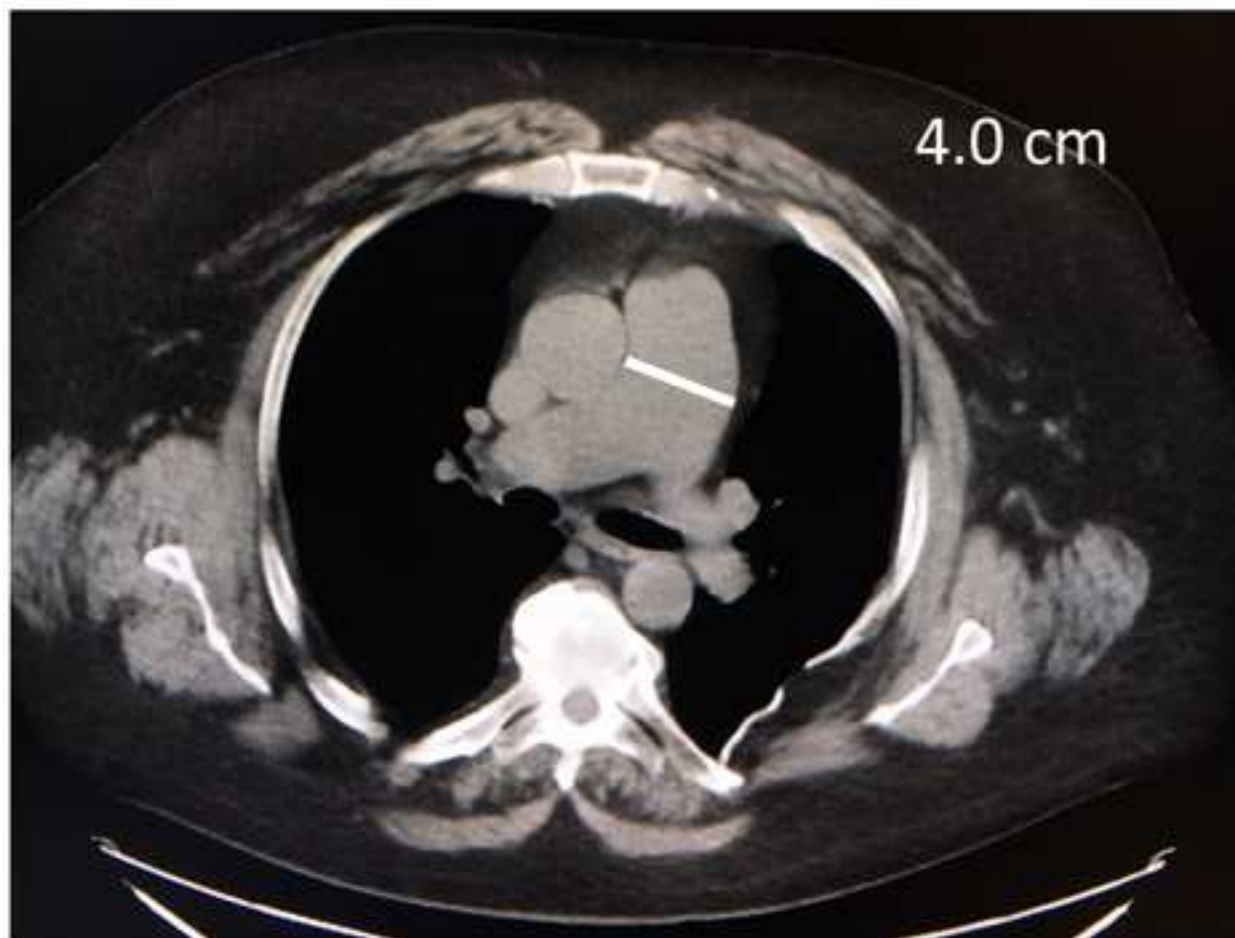


Figure 3

[Click here to access/download;Figure;Mets Figure 3 RCA infarct scar on NCCT axial and short axis.tif](#)







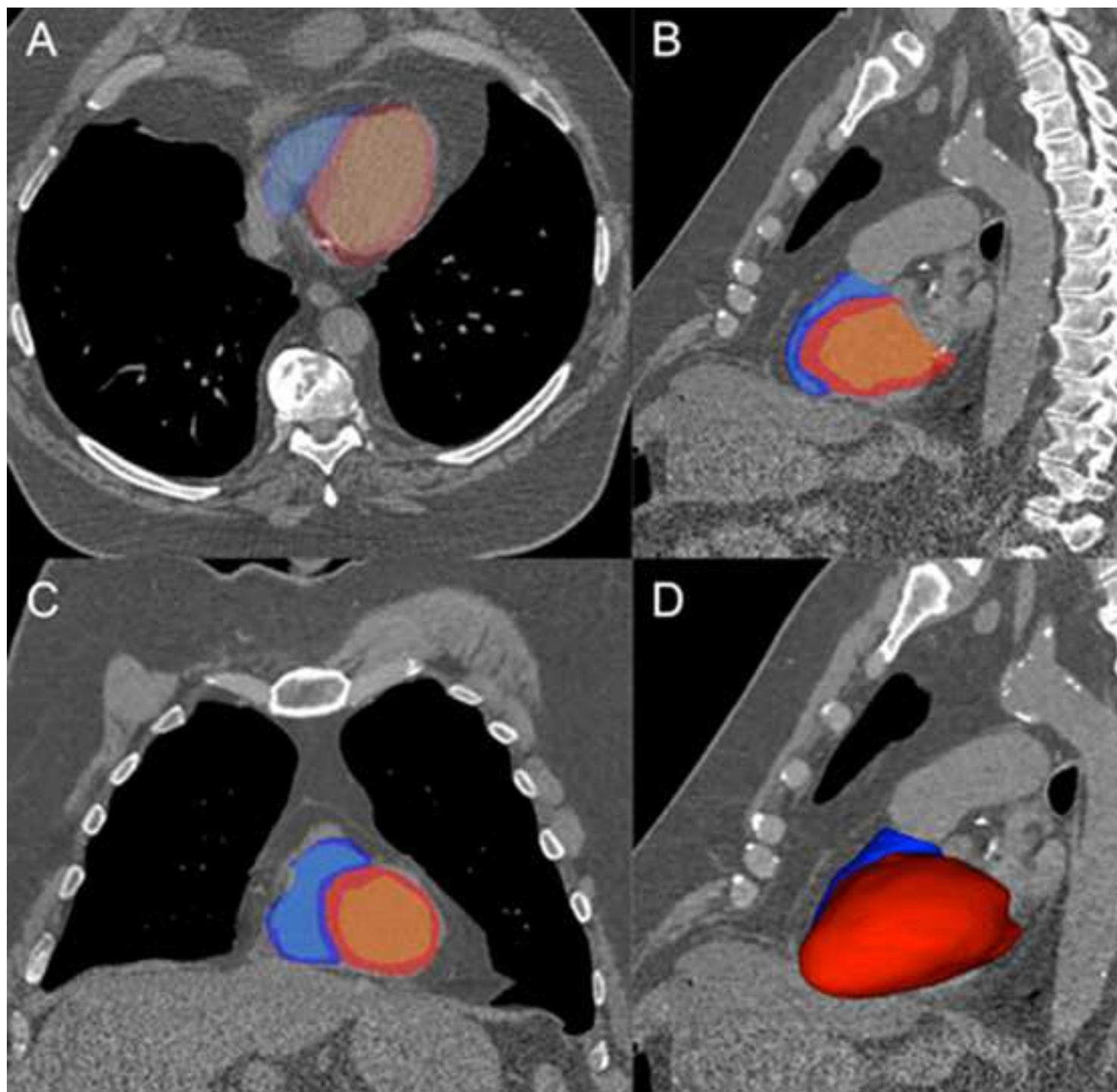


Table 1:

	Agatston Score	Visual Score (0-12)	Prognosis	Recommendation	Comment
No CAC	0	0	More favorable prognosis for CV events;	The presence of chronic obstructive CAD is very unlikely, life style changes	Might be false negative since small calcific lesions are missed (Agatston score <10): the visual score is less sensitive in subjects with low CAC burden
Mild CAC	1-100	1-4	Mildly increased risk for CV event	Consider further coronary evaluation and primary preventive treatment according to the patient global risk, life style changes should be more emphasized.	
Moderate CAC	101-400	5-7	Mildly increased risk of CV event	Consider further coronary evaluation and primary preventive treatment according to the patient global risk and clinical manifestations; in patients with Framingham risk intermediate and above ($\geq 10\%$ in 10 years) statin should be considered.	
Severe CAC	>400	8-12	Significantly increases the CV risk and total mortality	In asymptomatic subjects, consider further coronary evaluation by stress ECG, stress echo or SPECT imaging to R/O obstructive CAD; statin therapy should be highly considered.	Mostly prevalent in old patients and in those with clinical CAD, PVD and renal failure

Table 1: Importance of coronary artery calcification found on non-cardiac gated chest computed tomography in patients that smoke cigarettes (table modified from Shemesh et al) (70) Practical comments for chest radiologists showing that the larger ordinal coronary artery calcium score is associated with an increased risk of Major Adverse Cardiac Events. (This table is modified from Shemesh et al (70)) Abbreviations: CAC- coronary artery calcium score; Visual Score (Likert Scale range from 0-12); CAD- coronary artery disease, PVD- peripheral vascular disease;

Table 2

Non contrast, Chest CT finding	Index cases(n)/ Normal Values (N) [n/N]	Abnormal Value [n/N]	Unadjusted Hazard Ratio For MACE or Death (95% C.I) _p value_	Adjusted Hazard Ratio (95% CI) _p value_	Reference
Heart					
Transverse diameter of heart					Leiner article
Left Atrial Index, mm ² /m ²	917 ±187 [3389/3630]	992 ± 214 [241/3630]	1.42 (1.27-1.59) _<0.0001_	1.18 (1.02- 1.37) _0.023_	Gated exam Mahabadi 2016
Left Ventricular Index, mm ² /m ²	2,146 ± 275 [3389/3630]	2,240 ± 305 [241/3630]	1.36 (1.21-1.52) _<0.0001_	1.08 (0.93- 1.25) _0.31_	Gated exam Mahabadi 2016
Epicardial Fat Volume, ml	92.7 ± 46.0 [3389/3630]	117.5 ± 55.6 [241/3630]	1.52 (1.38-1.68) _<0.0001_	1.18 (1.02- 1.34) _0.023_	Gated exam Mahabadi 2016 <0.0001
Ascending or Descending Aortic Calcification	Ca++ present 61.5% [2083/3630]	Ca++ present 77.2% [186/241]	2.08 (1.54-2.81) _0.0001_	1.14 (0.83- 1.57) _0.41_	Gated exam Mahabadi 2016 (<0.0001)
Aortic Valve Calcifications	Ca++ Present 10.3% [324/3,389]	Ca++ Present 19.9% [48/241]	2.34 (1.7-3.2) _0.0001_	1.03 (0.73- 1.44) _0.88_	Gated exam Mahabadi 2016
Ascending Aortic Diameter at Pul Art bifurcation	35.5 ± 4.0 [3389/3630]	37.1 ± 4.1 [241/3630]	1.44 (1.29-1.61) _0.0001_	1.02 (0.94- 1.06) _0.25_	Gated exam Mahabadi 2016
Descending Aortic Diameter (mm) at Pul Art bifurcation	26.5 ±2.9 [3389/3630]	27.9 ±2.7 [241/3630]	1.56 (1.39-1.76) _<0.0001_	0.94 (0.88- 1.03) _0.06_	Gated exam Mahabadi 2016
Mitral Valve Leaflet Calcium					Andreas H. Mahnken1,2

Mitral Valve Annulus Calcium	2.4% [76/3,389]	4.2% [10/241]	1.9 (1.01-3.58) _0.0001_	0.73 (0.38- 1.40) _0.34_	Gated exam Mahabadi 2016
---------------------------------	--------------------	------------------	--------------------------------	-----------------------------------	--------------------------------

Legend Table 2: Imaging findings on non-contrast, non-cardiac gated Chest Computed tomography exams that are reflective of individual biology and the metabolic syndrome. (Abbreviations: n- number affected. N=total in study)

Table 3

NCCT imaging Finding	Absent Score=0	Mild Score=1	Moderate Score=2	Severe Score=3
Left anterior descending coronary artery calcification	none	1 or 2 calcified plaques limited to 2 or fewer images	Greater than 2 focal plaques or calcification extending for more than 2 slices	Fully calcified coronary artery extending for more than 3 slices
Descending Thoracic Aorta Calcification	none	Less than or equal to 3 focal calcified plaques	4-5 focal calcified plaques or one plaque extending for 3 or more slices	More than 5 focal calcified plaques or 2 plaques extending beyond 3 slices
Mitral valve leaflet Calcification	none	One leaflet calcified	Two leaflets calcified	

Legend Table 3: Imaging based cardiovascular risk biomarkers derived from a Caucasian population in Scotland (N= 2124) (71). This type of analytic approach to documenting vascular calcifications was first used by Jairam et al in 2014 (36).

Table 4

Model feature	Hazard Ratio	P value
Male	1.41	<0.001
Descending Aorta Calcification	1.45	<0.001
Mitral Valve Calcification	1.25	<0.001
LAD Calcification	1.11	<0.003
(Maximum Transverse Cardiovascular diameter in cm - 11cm) ²	1.03	<0.001
Age	1.03	<0.001

Legend Table 4: Hazard Ratios for the most significant model parameters for determining cardiovascular risk from contrast enhanced, non-gated chest CT exams from the PROVIDI study (N=10,410) (36).

Table 5

Model feature	Hazard Ratio Adjusted for FR score, CAC score and Multiple CT measures (95% C.I.)	P value
Left atrial index	1.21 (1.07-1.36)	0.002
Left ventricular index	1.15 (1.02-1.29)	0.02
Epicardial Fat Volume	1.14 (1.01-1.28)	0.04
<i>Presence of Thoracic Aortic Calcification</i>	1.14 (0.83-1.56)	0.43
<i>Diameter of Ascending aorta</i>	0.98 (0.84-1.15)	0.25
<i>Aortic Valve Calcification</i>	1.01 (0.72-1.40)	0.98
<i>Diameter of the Descending thoracic Aorta</i>	0.98 (0.84-1.15)	0.84
<i>Mitral Annulus Calcification</i>	0.81 (0.43-1.54)	0.81

Legend Table 5: Multivariable analysis of clinical and imaging based cardiovascular risk biomarkers derived from 3,630 subjects enrolled in the prospectively acquired Hienz-Nixdorff Recall Study. (37) and their adjusted Hazard Ratios for the interval development of major adverse cardiac events (MACE). (Abbreviations: FR- Framingham Risk Score, CAC- Coronary artery Agatston Score,)



[Click here to access/download](#)

Supplemental Data File (.doc, .tif, pdf, etc.)
Table S1.docx





[Click here to access/download](#)

Supplemental Data File (.doc, .tif, pdf, etc.)
Supplementary Table S2.docx





[Click here to access/download](#)

Supplemental Data File (.doc, .tif, pdf, etc.)
Supplementary Table S3.docx





[Click here to access/download](#)

Supplemental Data File (.doc, .tif, pdf, etc.)
Table S1 S2 and S3.docx

